A hemolytic pigment of Group B Streptococcus allows bacterial penetration of human placenta

Christopher Whidbey,[1,3,4] Maria Isabel Harrell,[3] Kellie Burnside,[1] Lisa Ngo,[3] Alexis K. Becraft,[3] Lakshminarayan M. Iyer,[5] L. Aravind,[5] Jane Hitti,[2] Kristina M. Adams Waldorf,[2] and Lakshmi Rajagopal[1,3,4]

[1]Department of Pediatric Infectious Diseases and [2]Department of Obstetrics and Gynecology, University of Washington School of Medicine, Seattle, WA 98195
[3]Center for Childhood Infections and Prematurity Research, Seattle Children's Hospital Research Institute, Seattle, WA 98101
[4]Department of Global Health, University of Washington School of Public Health, Seattle, WA 98195
[5]Computational Biology Branch, National Center for Biotechnology Information, National Institutes of Health, Bethesda, MD 20894

Microbial infection of the amniotic fluid is a significant cause of fetal injury, preterm birth, and newborn infections. Group B Streptococcus (GBS) is an important human bacterial pathogen associated with preterm birth, fetal injury, and neonatal mortality. Although GBS has been isolated from amniotic fluid of women in preterm labor, mechanisms of in utero infection remain unknown. Previous studies indicated that GBS are unable to invade human amniotic epithelial cells (hAECs), which represent the last barrier to the amniotic cavity and fetus. We show that GBS invades hAECs and strains lacking the hemolysin repressor CovR/S accelerate amniotic barrier failure and penetrate chorioamniotic membranes in a hemolysin-dependent manner. Clinical GBS isolates obtained from women in preterm labor are hyperhemolytic and some are associated with *covR/S* mutations. We demonstrate for the first time that hemolytic and cytolytic activity of GBS is due to the ornithine rhamnolipid pigment and not due to a pore-forming protein toxin. Our studies emphasize the importance of the hemolytic GBS pigment in ascending infection and fetal injury.

CORRESPONDENCE
Kristina Adams Waldorf:
adamsk@u.washington.edu
OR
Lakshmi Rajagopal:
lakshmi.rajagopal@
seattlechildrens.org

Abbreviations used: COSY, correlation spectroscopy; DTS, DMSO containing 0.1% TFA and 20% starch; ECIS, electric cell–substrate impedance sensing; GBS, Group B Streptococcus; hAEC, human amniotic epithelial cell; hRBC, human RBC; NMR, nuclear magnetic resonance.

Preterm birth is a major factor contributing to neonatal disease and accounts for 75% of perinatal mortality worldwide (Goldenberg et al., 2000). Currently, there is no effective therapy for prevention of human preterm births or stillbirths. Intra-amniotic infection and inflammation are important causes of preterm birth, stillbirth, fetal injury, and early onset neonatal sepsis (Watts et al., 1992; Goldenberg et al., 2000; Yoon et al., 2000; Lukacs et al., 2004; Behrman and Butler, 2007). Early onset sepsis in human newborns manifests within the first few hours of life, is fulminant, and is due to organisms acquired in utero with the amniotic fluid and neonatal blood infected with organisms commonly colonizing the lower genital tract such as Group B Streptococcus (GBS; Hillier et al., 1988; Romero et al., 1989c; Hillier et al., 1991; Puopolo, 2008; Gravett et al., 2010; Verani et al., 2010).

GBS are β-hemolytic, gram-positive bacteria that are a frequent cause of human newborn infections. Morbidities due to GBS infections include delayed development, vision and hearing loss, chronic lung disease, mental retardation, and cerebral palsy (Ledger, 2008). Despite the success of intrapartum antibiotic prophylaxis to prevent GBS transmission to the neonate during labor and delivery, in utero infections that occur earlier in pregnancy leading to stillbirth and preterm birth are not targeted by this approach and the burden of early onset sepsis in newborn infants remains substantial (Verani et al., 2010; Weston et al., 2011). Additional preventive therapies are urgently needed before the widespread use of antibiotics in pregnant women creates sufficient resistance such that our current antibiotics become ineffective.

C. Whidbey and M.I. Harrell contributed equally to this paper.

The Rockefeller University Press $30.00
J. Exp. Med. 2013 Vol. 210 No. 6 1265-1281
www.jem.org/cgi/doi/10.1084/jem.20122753

A key factor limiting preventive strategies is insufficient knowledge of virulence mechanisms that promote infection of the amniotic cavity. The human placenta is a critical multicellular organ that protects the growing fetus from organisms colonizing the lower genital tract. As the placenta is the most species-specific mammalian organ (Ala-Kokko et al., 2000; Hutson et al., 2011), no animal placenta recapitulates the exact mechanistic and physical barriers of the human placenta. The widely accepted route of pathogen entry into the human amniotic fluid requires bacterial ascension through the cervix and breach of several placental layers including the decidua, chorion, amnion, and amniotic epithelium (Bourne, 1960; Goldenberg et al., 2000). Although invasion of the amniotic epithelium is critical for pathogen entry into the amniotic cavity, previous studies have indicated that GBS do not invade human amniotic epithelial cells (hAECs) which constitute the amniotic epithelium (Winram et al., 1998). Consequently, mechanisms and virulence factors that mediate ascending GBS infection from the lower genital tract into the amniotic cavity and fetus are not understood.

RESULTS

Hemolysin promotes GBS invasion of hAECs

As GBS has been isolated from amniotic fluid of women with intact chorioamniotic membranes (Bobitt and Ledger, 1977; Naeye and Peters, 1978; Winram et al., 1998; Goldenberg et al., 2000), we investigated mechanisms that promote GBS invasion and breach of amniotic epithelium and chorioamnion. We hypothesized that intra-amniotic GBS infections in patients with intact placental or chorioamniotic membranes (Bobitt and Ledger, 1977; Naeye and Peters, 1978; Winram et al., 1998; Goldenberg et al., 2000) may be due to elevated virulence factor expression. The two component regulatory system CovR/S was described to repress the expression of many GBS virulence genes including genes of the *cyl* operon containing *cylE* important for the pluripotent toxin known as β-hemolysin/cytolysin (hereafter referred to as hemolysin; Lamy et al., 2004; Jiang et al., 2005; Rajagopal et al., 2006). To test if increased expression of virulence factors promotes GBS invasion of amniotic epithelium, we compared the ability of WT GBS and the hyper-hemolytic Δ*covR* to adhere to and invade hAEC. To evaluate the role of hemolysin, nonhemolytic GBS lacking the *cylE* gene associated with hemolysin production (Pritzlaff et al., 2001) were included (Δ*cylE* and Δ*covR*Δ*cylE*). The hemolytic activity of WT, hyper-hemolytic Δ*covR*, and nonhemolytic Δ*cylE* strains is shown in Fig. 1 A. Primary hAECs were isolated and cultured from normal, term placentas obtained immediately after cesarean delivery from women without labor and adherence and invasion of GBS to hAEC was determined as previously described (Winram et al., 1998; Lembo et al., 2010). Consistent with previous reports (Winram et al., 1998), we observed that WT GBS adhered to hAEC (Fig. 1 B). The presence or absence of CovR or CylE had no significant effect on GBS adherence to hAEC (Fig. 1 B, $P > 0.2$). However, in contrast to previous observations (Winram et al., 1998), we observed that WT GBS invaded hAEC (~4% invasion; Fig. 1 C). The Δ*cylE* mutant showed significantly decreased invasion when compared with WT (~0.3% invasion, $P = 0.008$; Fig. 1 C). Consistent with our hypothesis, we observed that the hyper-hemolytic GBSΔ*covR* was significantly more invasive to hAEC when compared with the WT (~80% invasion, $P < 0.0001$; Fig.1 C). Notably, the increase in hAEC invasion observed with GBSΔ*covR* was abolished in the absence of the gene *cylE* linked to hemolysin expression (Fig. 1 C, Δ*covR*Δ*cylE*). Collectively, these results indicate that hemolysin promotes GBS invasion of hAECs. Of note, the levels of GBS invasion observed with hAEC and differences between

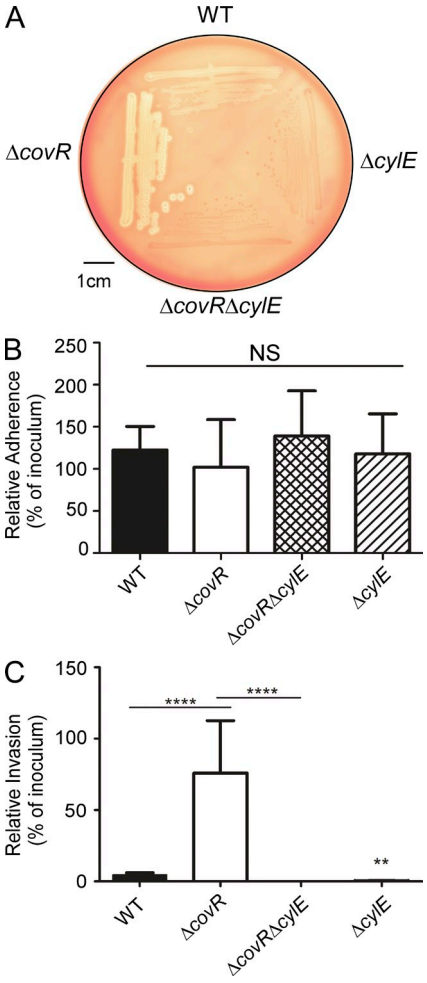

Figure 1. Hemolysin promotes GBS invasion of hAECs. (A) Hemolytic activity shown by the zone of clearing around the colonies on sheep blood agar of GBS WT, Δ*covR*, and isogenic mutants. A representative image from one of three independent experimental replicates is shown. (B and C) Primary hAECs were isolated from chorioamniotic membranes and adherence and invasion of GBS WT, isogenic Δ*covR*, Δ*covR*Δ*cylE*, and Δ*cylE* mutants were compared. Percent adherence (B) and invasion (C) is normalized to that of the initial inoculum. Data shown are the mean and SD obtained from hAECs that were isolated from four independent placentas, and each experiment was performed in triplicate (NS, $P > 0.2$; ****, $P < 0.0001$; **, $P = 0.008$, Student's *t* test, error bars ± SD).

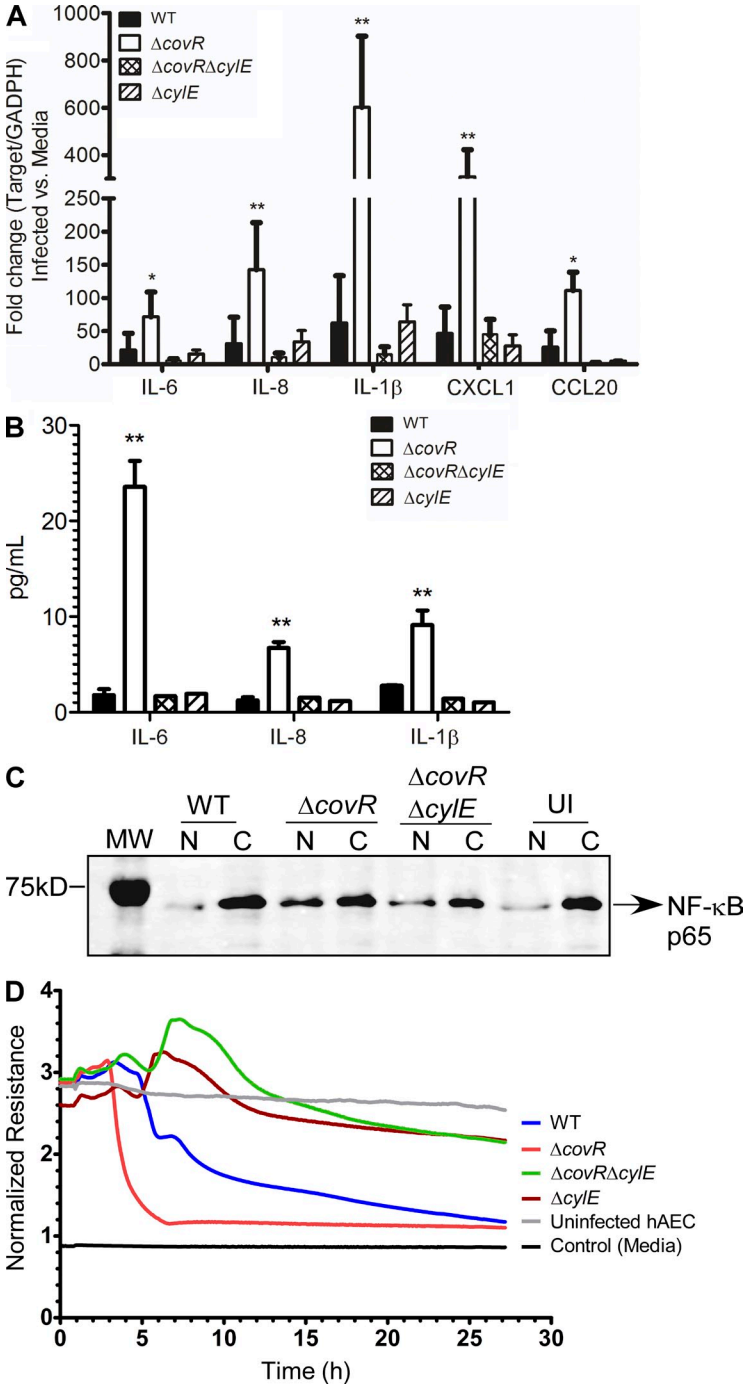

Figure 2. Hemolysin increases expression of inflammatory mediators and induces barrier disruption in amniotic epithelial cells. (A) qRT-PCR was performed of indicated cytokines/chemokines on RNA isolated from hAEC infected with either WT GBS COH1 or isogenic Δ*covR*, Δ*covR*Δ*cylE*, and Δ*cylE* mutants at 4 h after infection. Data shown are the mean and SD obtained from hAECs that were isolated from three independent placentas, performed in triplicate ($n = 3$; **, P = 0.007; *, P = 0.03, Student's *t* test, error bars ± SD). (B) Luminex bead assays were performed on supernatants of hAEC infected with WT GBS or isogenic Δ*covR*, Δ*covR*Δ*cylE*, and Δ*cylE* mutants at 4 h after infection. The experiment was performed using hAECs that were isolated from three independent placentas, performed in triplicate ($n = 3$; **, P < 0.005, Student's *t* test, error bars ± SD). (C) Western blots were performed on nuclear (N) and cytoplasmic (C) proteins from GBS-infected hAEC using antibody to NF-κB. Uninfected (UI) hAECs were included as controls. MW = molecular weight marker. A representative image from one of three independent experimental replicates is shown. (D) Barrier resistance of hAEC was monitored in real time using ECIS. A representative image from one of three independent experimental replicates is shown.

hypoinvasive and hyperinvasive strains is consistent with levels of GBS invasion reported in other cell types including human brain microvascular endothelial cells and lung epithelial cells (Doran et al., 2002, 2005; van Sorge et al., 2009).

Hemolysin induces activation of proinflammatory mediators in human amniotic epithelium

We examined if increased hemolysin in Δ*covR* activates an inflammatory response in human amniotic epithelium. To evaluate changes in expression of inflammatory genes in GBS-infected hAEC, qRT-PCR was performed on RNA isolated at 4 h after infection using previously described methods (Lembo et al., 2010). These results indicate that infection with Δ*covR* caused a significant increase in transcription of cytokines such as IL-6, IL-8, IL-1β, CXCL1, and CCL20 in hAEC compared with cells infected with the isogenic WT (COH1) or uninfected controls (Fig. 2 A). Interestingly, the increase in inflammatory gene expression observed with GBSΔ*covR* was abolished in hAEC infected with Δ*covR*Δ*cylE* (Fig. 2 A). Luminex bead assays confirmed that secretion

of IL-6, IL-8, and IL-1β was higher in Δ*covR*-infected hAEC compared with the WT GBS or Δ*covR*Δ*cylE* (Fig. 2 B, $P < 0.005$).

Hyper-hemolytic GBSΔ*covR* infection increases NF-κB recruitment into the nucleus of hAEC

Microbial toxins have been implicated in activating inflammatory signaling pathways via the nuclear transcription factor NF-κB, which is recruited from the cytoplasm to the nucleus during activation (Gonzalez et al., 2008). Therefore, we examined whether the increase in proinflammatory gene expression observed in hAEC infected with the hyper-hemolytic GBSΔ*covR* was associated with nuclear localization/recruitment of the transcription factor NF-κB. To test this hypothesis, total nuclear and cytoplasmic proteins isolated from infected and uninfected hAEC were resolved on 10% SDS-PAGE and Western blots were performed using antibody to NF-κB p65. The results shown in Fig. 2 C indicate that infection with Δ*covR* results in an ∼2.5-fold increase in recruitment of NF-κB into the nucleus of infected hAEC when compared with WT GBS or uninfected controls. These data confirm that the increase in inflammatory gene expression observed in Δ*covR*-infected hAEC is associated with increased nuclear recruitment of NF-κB.

Hemolysin promotes GBS breach of the human amniotic epithelial barrier

We next examined if hemolysin accelerates failure of the human amniotic epithelial barrier. Changes in transepithelial electrical resistance were monitored across hAEC monolayers in real time using electric cell–substrate impedance sensing (ECIS; Giaever and Keese, 1993). In brief, hAEC monolayers established on gold-plated electrodes in 8-well array slides were infected with GBS WT, isogenic Δ*covR*, Δ*covR*Δ*cylE*, or Δ*cylE* at 10^5 CFU/well as previously described (Lembo et al., 2010). Uninfected wells were included as controls. Fig. 2 D shows that the decrease in barrier resistance observed in hAEC infected with WT GBS was not observed in hAEC infected with the hemolysin-deficient strain Δ*cylE*. Furthermore, we observed that infection with Δ*covR* accelerated the decrease in barrier resistance compared with WT (Fig. 2 D). Notably, the rapid decrease in barrier resistance due to Δ*covR* was abolished in Δ*covR*Δ*cylE* (Fig. 2 D). These results suggest that increased hemolysin expression enables GBS to breach barrier function of the amniotic epithelium. We further observed that prolonged exposure of Δ*covR* to hAEC (>4 h) induced cytotoxic effects in contrast to hAEC exposed to GBS WT and Δ*cylE* strains. Collectively, these observations indicated that hemolysin is an important virulence factor that promotes bacterial invasion and immune activation of the amniotic epithelium leading to secretion of cytokines, such as IL-6, IL-8, and IL-1β, that have associated with preterm labor and neonatal morbidity (Romero et al., 1989a,b, 1990, 1991; Gotsch et al., 2007).

Hyper-hemolytic GBS penetrate human placenta/chorioamnion and can be associated with women in preterm labor

Ascending in utero infection of GBS from the lower genital tract into the amniotic cavity requires the pathogen to penetrate the chorioamniotic membranes. Thus, we tested the ability of GBS to penetrate intact membranes that were mounted and maintained on a modified transwell system as previously described (Zaga-Clavellina et al., 2007). 48 h after stabilization, intact chorioamniotic membranes ($n = 6$) were infected with 10^7 CFU of GBS (WT, Δ*covR*, and Δ*covR*Δ*cylE*) on the choriodecidual side of the placenta. Uninfected chorioamnion was included as controls. In parallel, we also examined the ability of GBS to penetrate either chorion alone or amnion alone, using the transwell model system (for details, see Materials and methods). At 24 h after infection, aliquots of media from the lower chamber were analyzed for bacterial CFU. As shown in Fig. 3 A, we observed that all GBS strains efficiently penetrated either the amnion or the chorion, as ≥10^8 CFU was recovered from the lower chamber of membranes infected with WT, Δ*covR*, and Δ*covR*Δ*cylE*. In contrast, no bacterial CFU was recovered from chorioamnion infected with WT or Δ*covR*Δ*cylE* (Fig. 3 A). Notably, ≥10^2 bacterial CFU were recovered from four of six chorioamniotic membranes infected with GBSΔ*covR* (Fig. 3 A, $P = 0.02$). Transverse histological sections of the infected chorioamnion were prepared and stained for bacteria as previously described (Stevens and Bancroft, 1977). Interestingly, bacterial invasion of the chorioamnion, including penetration of the amniotic epithelium, was observed in chorioamniotic membranes infected with the hyper-hemolytic GBSΔ*covR* even when bacteria were not recovered in the lower chamber (Fig. 3 B). In contrast, bacteria were primarily seen in the choriodecidual region in chorioamniotic membranes infected with WT and very few bacteria are observed in membranes infected with Δ*covR*Δ*cylE* (Fig. 3 B). Increased secretion of IL-6 was also observed in media obtained from the lower chamber of chorioamniotic membranes infected with Δ*covR* (Fig. 3 C, $P = 0.02$). We were unable to extend the experiments longer than 24 h after GBS infection as the placental membranes begin to destabilize at >75 h after cesarean section. Collectively, these data show that although chorioamniotic membranes serve as an effective barrier to prevent GBS trafficking, increased production of hemolysin can facilitate bacterial penetration of chorioamniotic membranes and the amniotic cavity.

We examined if increased hemolytic activity could be observed in GBS isolated from women in preterm labor. To this end, clinical isolates obtained from human amniotic fluid and chorioamnion were examined for their hemolytic properties and potential mutations in the *covR/S* locus. We obtained eight GBS strains that were isolated from six women enrolled in a cohort of women in preterm labor with intact membranes and where information on outcomes and microbiological cultures of the amniotic fluid, chorioamnion, and cord blood were available (Hitti et al., 1997; see Table 1). Most of these GBS isolates exhibited increased hemolytic activity and increased transcription of genes in the *cyl* operon such as *cylE* (Figs. 4, A and B). DNA sequencing indicated the presence of mutations in the *covR/S* loci in six isolates obtained from four women (Table 1). GBS isolated from both the amniotic fluid and chorioamnion of one patient in preterm labor

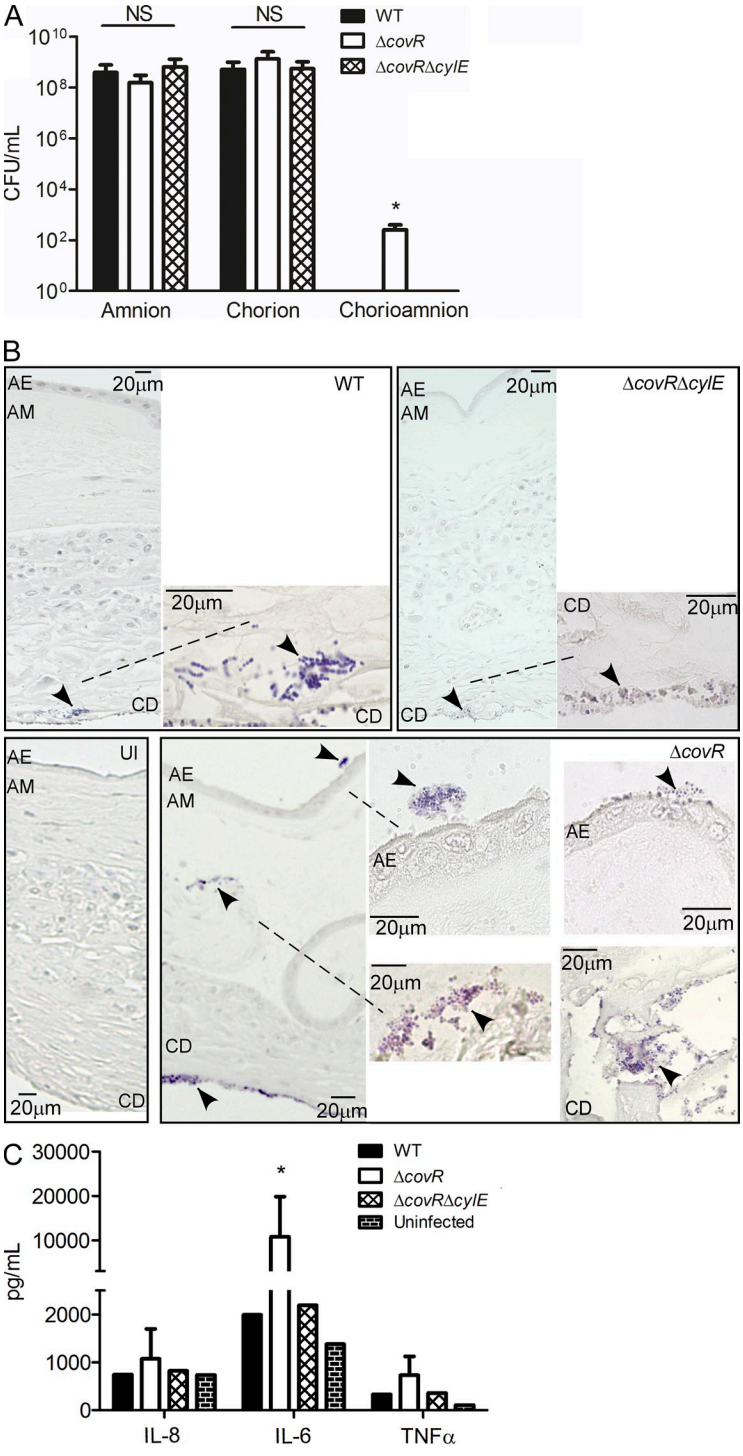

Figure 3. Hyper-hemolytic GBS penetrate human chorioamnion. Intact chorioamniotic membranes as well as either chorion alone or amnion alone ($n = 6$) were mounted on a transwell system and infected with either WT GBS COH1 or isogenic Δ*covR* and Δ*covR*Δ*cylE* strains for a period of 24 h. Aliquots of the media from the lower chamber were analyzed for CFU and cytokines expression (see A–C). (A) GBS penetration of the chorion, amnion, or chorioamniotic membranes ($n = 6$; NS, $P > 0.3$; *, $P = 0.02$, Mann Whitney test, error bars ± SD). (B) Infected chorioamniotic membranes ($n = 6$) were fixed, embedded, sectioned, and stained using Gram-Tworts stain. A representative placenta where bacteria were not recovered from the lower chamber for any GBS strain is shown. AE, amniotic epithelium; AM, amniotic mesoderm; CD, choriodecidua; UI, uninfected chorioamnion. Arrows represent gram-positive bacteria, and dashed line shows region under higher magnification. (C) ELISA assays on media obtained from the lower chamber of chorioamniotic membranes infected with GBS WT, Δ*covR*, and Δ*covR*Δ*cylE* ($n = 6$; *, $P = 0.02$, Mann Whitney test, error bars ± SD).

had a stop codon mutation in the kinase domain of CovS (CovS220Stop; Table 1). GBS isolated from amniotic fluid and cord blood of another patient in preterm labor had a valine to methionine substitution in CovS at position 343; the same mutation was also observed in a GBS isolate obtained from the amniotic fluid of a third patient (Table 1). GBS from amniotic fluid of another woman in preterm labor had a deletion in the promoter of *covR/S* (Table 1). Of note, two GBS isolates recovered from women in preterm labor had no mutations in the *covR/S* loci, and thus increased hemolytic activity and transcription of *cyl* genes (Fig. 4, A and B) may be mediated by other regulators of GBS hemolysin.

To determine if the identified CovR/S mutations affect hemolytic activity of GBS, we generated site-directed mutants. As shown in Fig. 4 C, GBSΔ*covR* and Δ*covS* strains

Table 1. GBS clinical isolates associated with preterm labor and mutations in *covR/S* locus

Isolate number[a]	Source	Mutation in *covR/S* loci[b]	Gestational age at birth[c]
1	Amniotic fluid	Deletion of adenine residue at position 658 in *covS* resulting in truncation of CovS at amino acid 220 (CovS 220Stop)	30 wk
1	Chorioamnion	Same as above *i.e.* CovS 220Stop	30 wk
2	Amniotic fluid	Deletion of 4 nucleotides 'ATTT' spanning -110 to -107 upstream to the ATG start codon in the promoter region of *covR/S*	34 wk
3	Amniotic fluid	Substitution of adenine instead of guanine resulting in amino acid substitution from valine to methionine in CovS (CovS V343M)	26 wk
3	Blood	CovS V343M	26 wk
4	Chorioamnion	CovS V343M	36 wk
5	Chorioamnion	None	36 wk
6	Chorioamnion	None	28 wk

[a]In some patients, GBS were isolated from two different locations, and both these isolates had the same mutation in *covR/S*.
[b]Only nonsynonymous changes are reported.
[c]All women enrolled in the study had preterm labor with intact membranes at ≤34 wk of gestation.

exhibit increased hemolytic activity when compared with the WT and complementation with plasmids that constitutively express either CovR or CovS restored repression of hemolytic activity to WT levels or greater. However, complementation of Δ*covS* with the plasmid encoding CovS220Stop failed to restore repression of hemolytic activity and partial complementation was observed with CovSV343M (compare Δ*covS*/pCovS to Δ*covS*/CovS220stop and Δ*covS*/CovSV343M in Fig. 4 C). Further studies are necessary to understand the role of this substitution in CovS signaling. Similarly, the presence of the promoter deletion in *covR/S* on the chromosome of WT GBS alleviated CovR repression of hemolysin (Fig. 4 C) and is consistent with our previous observations that CovR can positively regulate its own expression (Lembo et al., 2010). These results suggest that the increased hemolytic activity observed in the clinical isolates with CovR/S mutations can, at least in part, be attributed to these mutations. However, as GBS has an open pan-genome (Tettelin et al., 2005), the effect of other strains specific regulators cannot be ruled out. We further confirmed that, similar to Δ*covR*, GBSΔ*covS* showed increased invasion and accelerated barrier disruption of hAEC (Figs. 4, D and E). Complementation of Δ*covR* and Δ*covS* decreased amniotic epithelial invasion at levels similar to WT (Fig. 4 D) as did the complemented Δ*cylE* strain (not depicted). Although we were unable to complement the Δ*covR*Δ*cylE* double mutant due to the instability of the complementing plasmid, introduction of the plasmid encoding CylE to GBSΔ*covR*Δ*cylE* restored hemolytic activity, amniotic epithelial invasion, and barrier disruption to levels that were intermediate between WT and Δ*covR* (Figs. 4, C–E).

CylE expression is necessary but not sufficient for GBS hemolysis

Our results above add to the large body of literature demonstrating the essential nature of hemolysin to various facets of GBS pathogenesis including pneumonia, sepsis, meningitis (Liu et al., 2004; Hensler et al., 2005; Lembo et al., 2010), and now bacterial penetration of human placenta/chorioamnion. Despite the importance of hemolysin to GBS virulence, its biochemical and molecular nature has remained elusive. Extraction of the GBS hemolysin requires high molecular weight stabilizers such as starch, tween, or BSA (Marchlewicz and Duncan, 1980; Tapsall, 1987). Previous studies proposed that the 78-kD protein encoded by the *cylE* gene located in the *cyl* operon (Fig. 5 A) is the GBS hemolysin, as deletion of the *cylE* gene abolished hemolytic activity and expression of *cylE* increased hemolysis in *E. coli* (Pritzlaff et al., 2001). However, Pritzlaff et al. (2001) also reported that in *E. coli* expressing CylE, they could not detect the CylE protein in secreted/extracellular fractions and also could not extract hemolytic activity from the bacterial cells using starch, BSA, or tween, characteristic of the GBS hemolysin. These observations suggest that increased hemolytic activity in *E. coli* may not be a result of the GBS hemolysin. Also noteworthy is that CylE has 43 rare codons that are not efficiently translated in *E. coli* (i.e., 24 Arg [AGG, AGA, CGA], 5 Leu [CTA], 11 Ile [ATA], and 3 Pro [CCC]). BLAST searches have revealed no significant homology of CylE to known pore-forming toxins and the protein does not possess any canonical secretion signal (Pritzlaff et al., 2001; Nizet, 2002). Moreover, SDS-PAGE analysis of cell-free extracts of GBS with hemolytic activity did not reveal the presence of any protein (unpublished data). To further confirm that *cylE* alone is necessary and sufficient for GBS hemolysis, we constructed a GBS strain that lacked all genes of the *cyl* operon (Δ*cylX-K*, see Fig. 5 A for operon). This strain is nonhemolytic and, interestingly, complementation with plasmids that constitutively express either CylE or CylABE (which includes the ABC transporter system CylA/B; Gottschalk et al., 2006) failed to restore hemolytic activity (Fig. 5 B). In contrast, these plasmids restored hemolytic activity to the GBS strain lacking only *cylE* (Fig. 5 B) but were unable to induce hemolysis in *E. coli* (Fig. 5 C). Consistent with these observations, complementation of GBSΔ*covR*Δ*cylE* with pCylE restored hemolytic activity

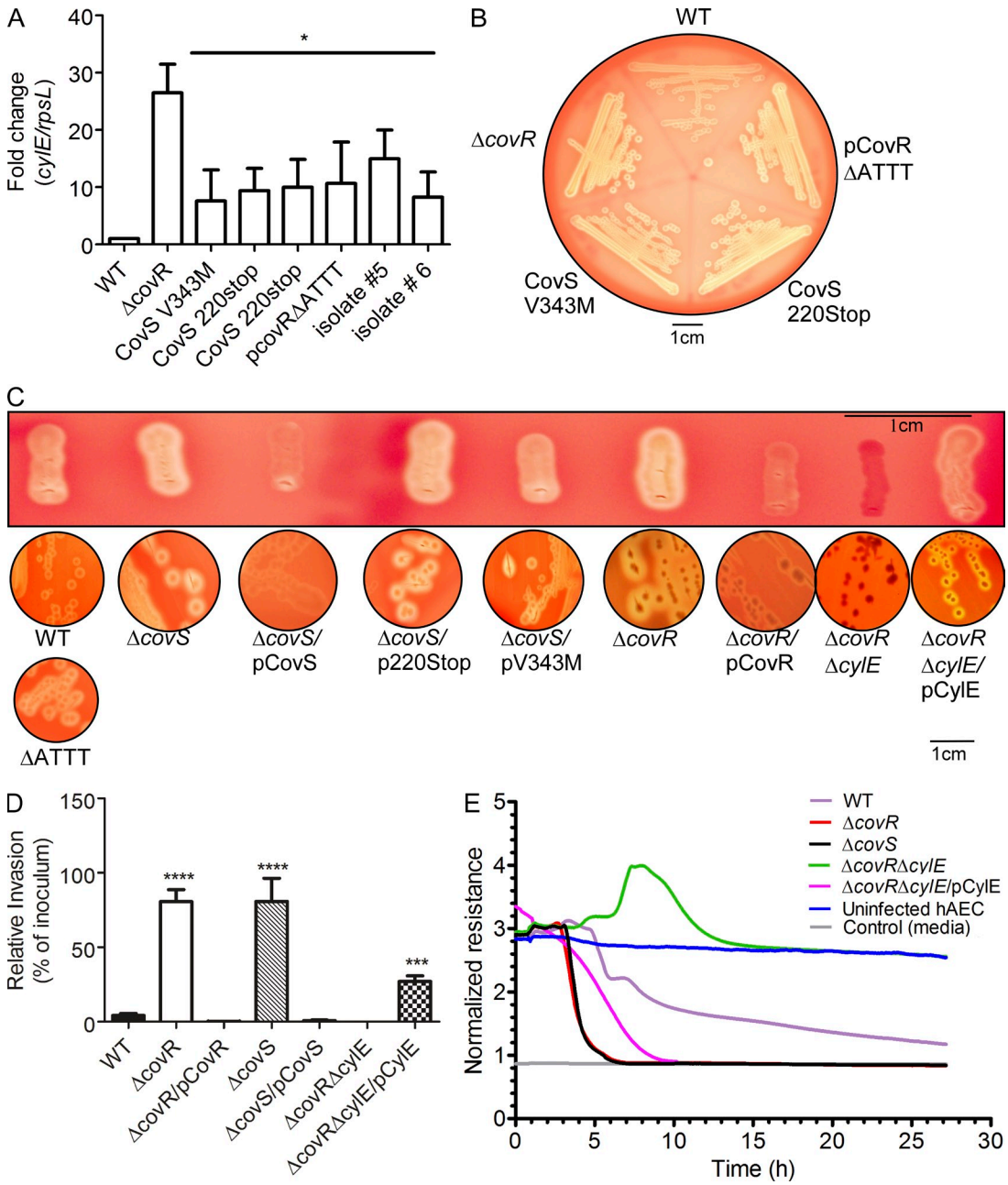

Figure 4. GBS clinical isolates from women in preterm labor exhibit increased hemolysis and some are associated with CovR/S mutations. (A) qRT-PCR on RNA isolated from log phase GBS ($0.D_{600nm}$ = 0.3). Data are normalized to relative expression of the house keeping gene *rpsL* and are the mean and SD from five independent biological replicates performed in triplicate (n = 5; *, P = 0.03, Wilcoxon matched-pairs rank test). (B) Hemolytic activity of GBS clinical isolates associated with preterm labor. A representative image from one of three independent experimental replicates is shown. (C) Single colonies were patched and streaked on blood agar. Hemolysis of GBS WT, Δ*covS*, Δ*covR*, and complementing clones including plasmids encoding CovS220stop and CovSV343M. Hemolysis of GBS with the pCovR promoter deletion compared with WT. Complementation of GBSΔ*covR*Δ*cylE* with pCylE on hemolytic activity. A representative image from one of three independent experimental replicates is shown. (D) Invasiveness of GBSΔ*covS* to hAEC compared with WT and Δ*covR*. Complementation of Δ*covS* and Δ*covR* on amniotic invasion and effect of pCylE on amniotic epithelial invasion of Δ*covR*Δ*cylE*. Data shown are the mean and SD obtained using hAEC from three independent placentas, performed in triplicate (n = 3; ****, P < 0.0001; ***, P = 0.0006, Student's t test, error bars ± SD). (E) Barrier disruption of amniotic epithelium by GBS WT, Δ*covS*, Δ*covR*, and Δ*covR*Δ*cylE*. Complementation of GBSΔ*covR*Δ*cylE* with pCylE on amniotic barrier disruption. A representative image from one of three independent experimental replicates is shown.

to levels greater than WT (Fig. 4 C) due to derepression of the other *cyl* operon genes in the absence of CovR (Lamy et al., 2004; Jiang et al., 2008; Lembo et al., 2010). Collectively, these observations indicate that although necessary, CylE and its putative transporter CylA/B are not sufficient for GBS hemolytic activity.

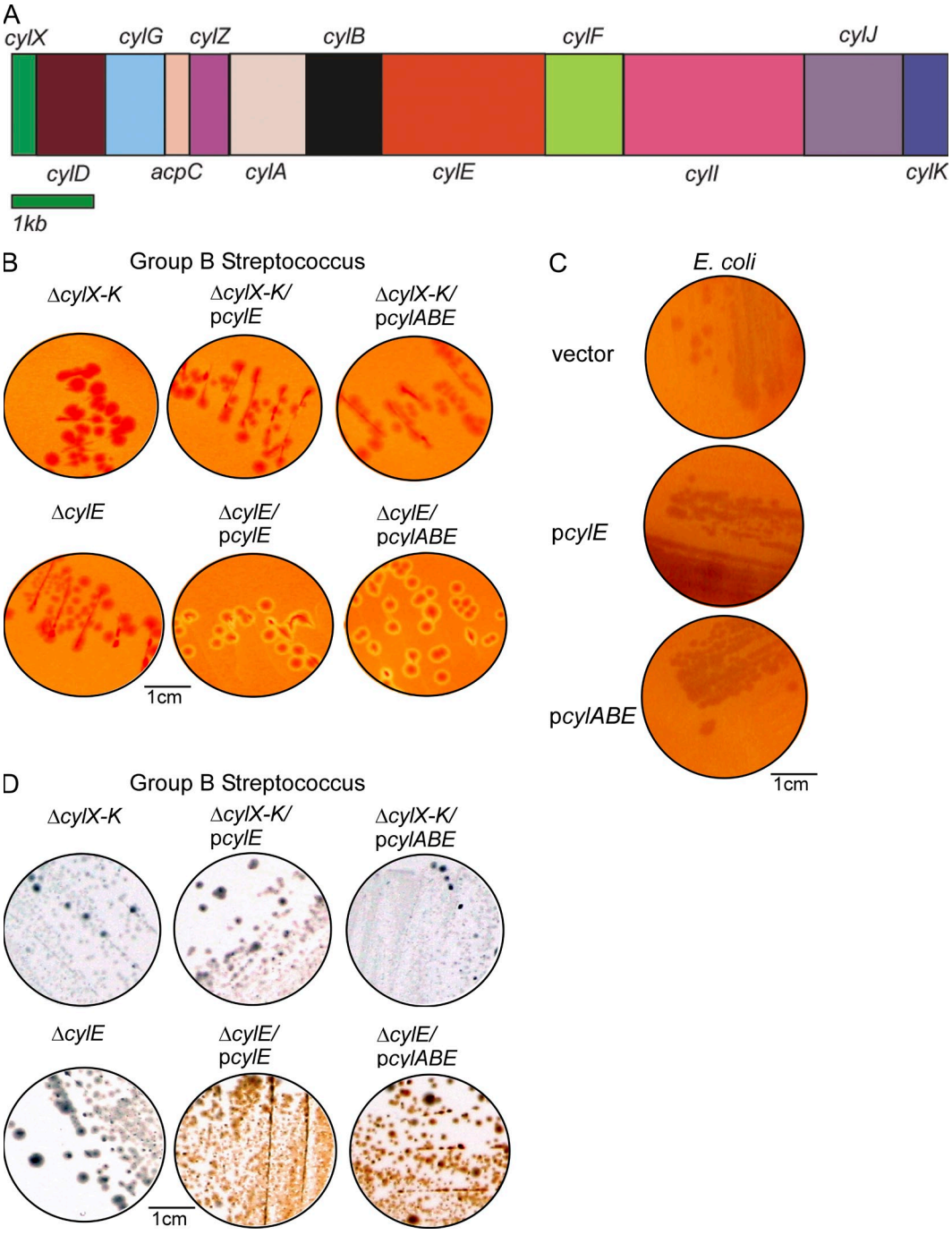

Figure 5. CylE is necessary but not sufficient for GBS hemolysis. (A) The GBS *cyl* operon encoding genes *cylX-K* is shown. (B and C) Complementation of the nonhemolytic GBSΔ*cylE* and Δ*cylX-K* with plasmids encoding CylE or CylE along with the ABC transporter CylA/B on hemolytic activity. A representative image from one of three independent experimental replicates is shown. (D) Hemolytic and nonhemolytic GBS strains on Granada Media. A representative image from one of three independent experimental replicates is shown.

The functional basis of GBS hemolytic activity is the ornithine rhamnolipid pigment

Although the hemolytic phenotype of GBS anomalously correlates with pigmentation, where nonhemolytic strains are nonpigmented and hemolytic strains are pigmented (Nizet et al., 1996; Spellerberg et al., 2000; Pritzlaff et al., 2001; also see Fig. 5 D), this link is not understood. The pigment was recently described to be an ornithine rhamnolipid known as granadaene (Rosa-Fraile et al., 2006). Like hemolytic activity, pigment biosynthesis in GBS requires the 12-gene *cyl* operon (Spellerberg et al., 2000; Pritzlaff et al., 2001; Fig. 5 A) and several genes in this operon (*cylD*, *cylG*, *cylI*, *cylK*, *cylZ*, and

A

Gene	Predicted Function	Gene	Predicted Function
cylX	Acetyl CoA carboxylase	*cylB*	ABC transport
cylD	Malonyl-CoA-ACP transacylase	*cylE*	N-acyltransferase
cylG	3-ketoacyl-ACP reductase	*cylF*	Aminomethyltransferase
acpC	Acyl carrier protein	*cylI*	3-ketoacyl-ACP synthase
cylZ	β-hydroxy-ACP dehydratase	*cylJ*	Glycosyltransferase
cylA	ABC transport	*cylK*	Phosphopantetheinyl transferase

B

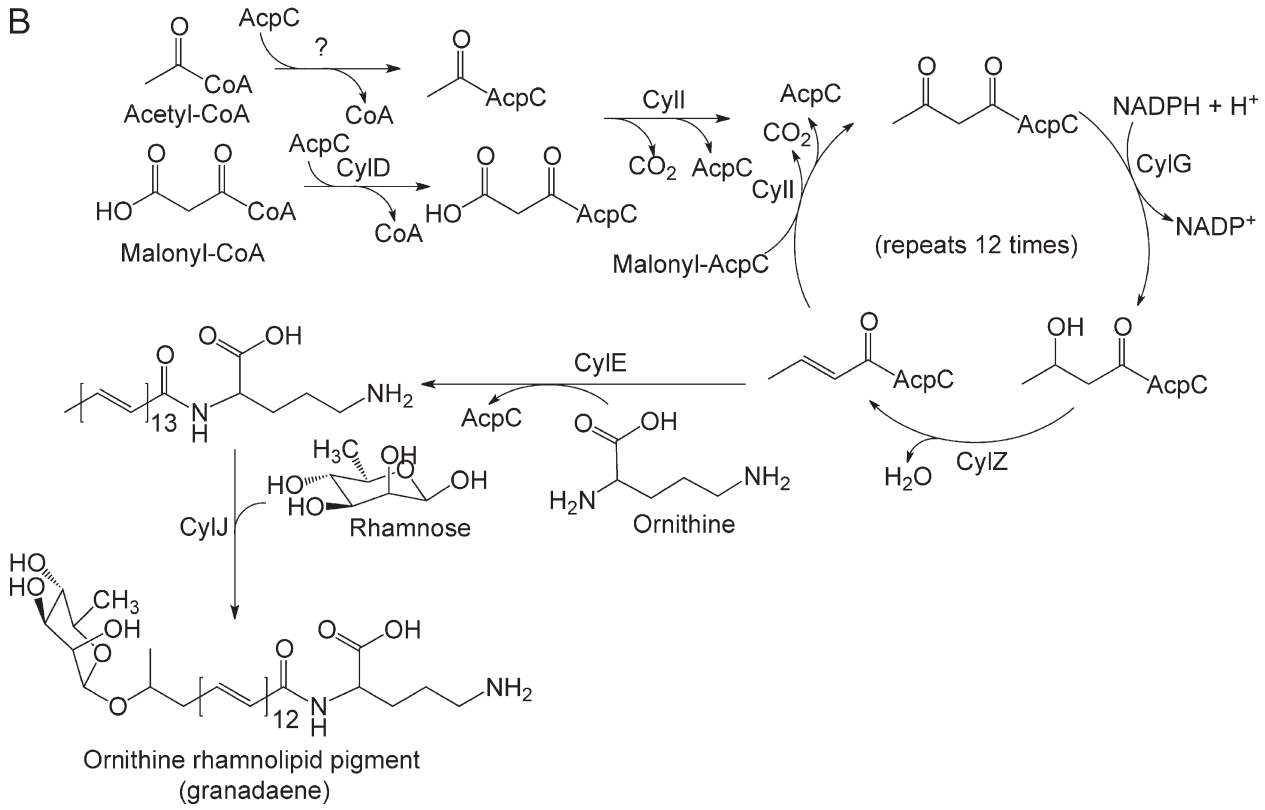

Figure 6. Proposed biosynthetic pathway for the GBS pigment granadaene. (A and B) Predicted functions of the *cyl* operon proteins and proposed biosynthetic pathway for synthesis of the GBS pigment using acetyl-CoA, malonyl-CoA, ornithine, and rhamnose. CylD conjugates the elongating malonyl CoA units to the acyl carrier protein (ACP) AcpC. CylI links the malonyl CoA to an initial fatty acid–ACP complex, beginning the fatty acid biosynthesis-like pathway. CylG reduces the 3-keto group to a hydroxyl group, which is further reduced to an alkene by CylZ. The *cyl* operon lacks an enoyl-ACP reductase thereby eliminating the final reduction of the alkene to an alkane. The unsaturated fatty acid serves as a substrate for further elongation by CylI, accounting for the large degree of unsaturation in the pigment. After 13 total rounds of elongation, the fatty acid is conjugated to ornithine by CylE, and glycosylated by CylJ. CylX, CylF, and CylK likely function upstream or downstream of this pathway. CylX is homologous to a component of the acetyl-CoA carboxylase, which generates malonyl-CoA. CylF is an aminomethyltransferase, likely involved in production of the methylated derivative seen in the mass spectrum (Fig. S2). CylK is a putative phosphopantetheinyl transferase, which is involved in the activation of acyl carrier proteins. Although GBS has a separate fatty acid biosynthesis (*fab*) operon, deletion of genes in the *cyl* operon (Δ*cylX-K*, Fig. 5B) abolishes pigment biosynthesis suggesting that the *fab* and *cyl* operons are not functionally redundant.

acpC) encode enzymes catalyzing different steps in fatty acid biosynthesis (Fig. 6 A). The *cyl* operon also encodes a glycosyltransferase (CylJ), an aminomethyltransferase (CylF), acetyl CoA carboxylase (CylX), and an ABC transporter (CylA/B). Sequence profile analysis of CylE revealed an N-terminal domain of the acyltransferase superfamily known to catalyze several amidoligase reactions (Fig. S1). Using these predicted homologies, a pathway for GBS pigment biosynthesis that requires most genes of the *cyl* operon is proposed (Fig. 6 B).

Based on the tight link between hemolysin and pigment production, the failure of *cylE* or *cylABE* to restore hemolytic activity to GBSΔ*cylX-K*, the absence of protein in the hemolytic extracts, and observations that disruption of several other *cyl* genes such as *cylD*, *acpC*, *cylZ*, *cylA/B*, and *cylK* abolished hemolytic activity (Spellerberg et al., 1999; Pritzlaff et al., 2001; Gottschalk et al., 2006; Forquin et al., 2007), we hypothesized that hemolytic activity of GBS may be due to the ornithine rhamnolipid pigment and not due to the CylE protein. To test this hypothesis, we extracted the pigment from WT GBS using DMSO containing 0.1% TFA as previously described (Rosa-Fraile et al., 2006). Subsequently, the pigment was purified by gel filtration column chromatography designed for

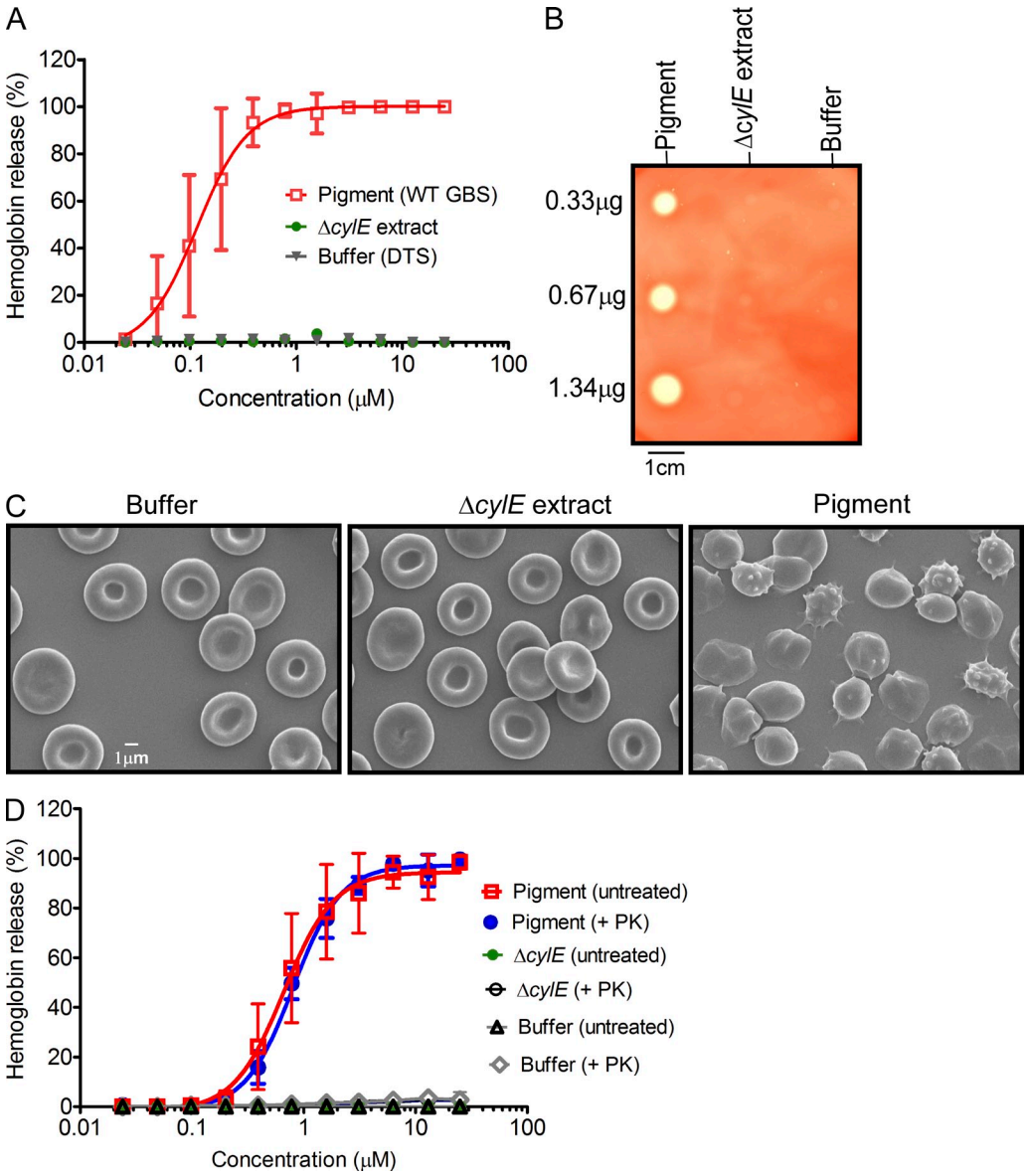

Figure 7. The functional basis of GBS hemolytic activity is the pigment. (A) Pigment was added to hRBCs in twofold serial dilutions from 25 to 0.024 μM. As controls, equivalent amounts of sample from Δ*cylE* or DTS were added to hRBC. The data shown are the mean and SD from three independent pigment preparations, performed in triplicate ($n = 3$, $P < 0.0001$ Student's *t* test, error bars ± SD). (B) Varying amounts of purified GBS pigment (0.33, 0.67, and 1.34 μg) was spotted on sheep blood agar plates and incubated overnight at 37°C. Equivalent amounts (2, 1, and 0.5 μl) of purified extract from GBSΔ*cylE* and DTS were spotted as controls. A representative image from one of three independent experimental replicates is shown. (C) Scanning electron micrographs showing hRBC membrane morphology after a brief (8 min) exposure to GBS pigment (12.5 μM) or an equal amount of control (buffer or Δ*cylE* extract). The experiment was performed twice using independent pigment preparations. (D) For proteinase K (PK) treatment of pigment before hemolytic assays, pigment, and control Δ*cylE* samples in DTS were lyophilized and digested in the presence and absence of proteinase K. The data shown are the mean and SD from three independent pigment preparations, performed in triplicate ($n = 3$, $P \geq 0.9$ Student's *t* test, error bars ± SD).

selective purification of small molecules (<5 kD) using a Sephadex LH-20 column and DMSO:0.1% TFA as the mobile phase (Rosa-Fraile et al., 2006). Although soluble in DMSO:0.1% TFA, the pigment was nonhemolytic in this solvent as observed previously (Rosa-Fraile et al., 2006). Because traditional isolation of GBS hemolytic extracts requires a large carrier molecule such as starch (Marchlewicz and Duncan, 1980; Tapsall and Phillips, 1991), we reasoned that addition of starch to the purified pigment may be required for functional activity. Thus, we dissolved purified pigment in DMSO containing 0.1% TFA and 20% starch (DTS). As a control, the pigment extraction procedure was performed on the nonhemolytic and nonpigmented Δ*cylE* strain. We then examined hemolytic activity of purified pigment using two methods that involved lysis of RBCs. First, twofold dilutions of pigment were used to examine lysis of human RBCs (hRBCs) using the

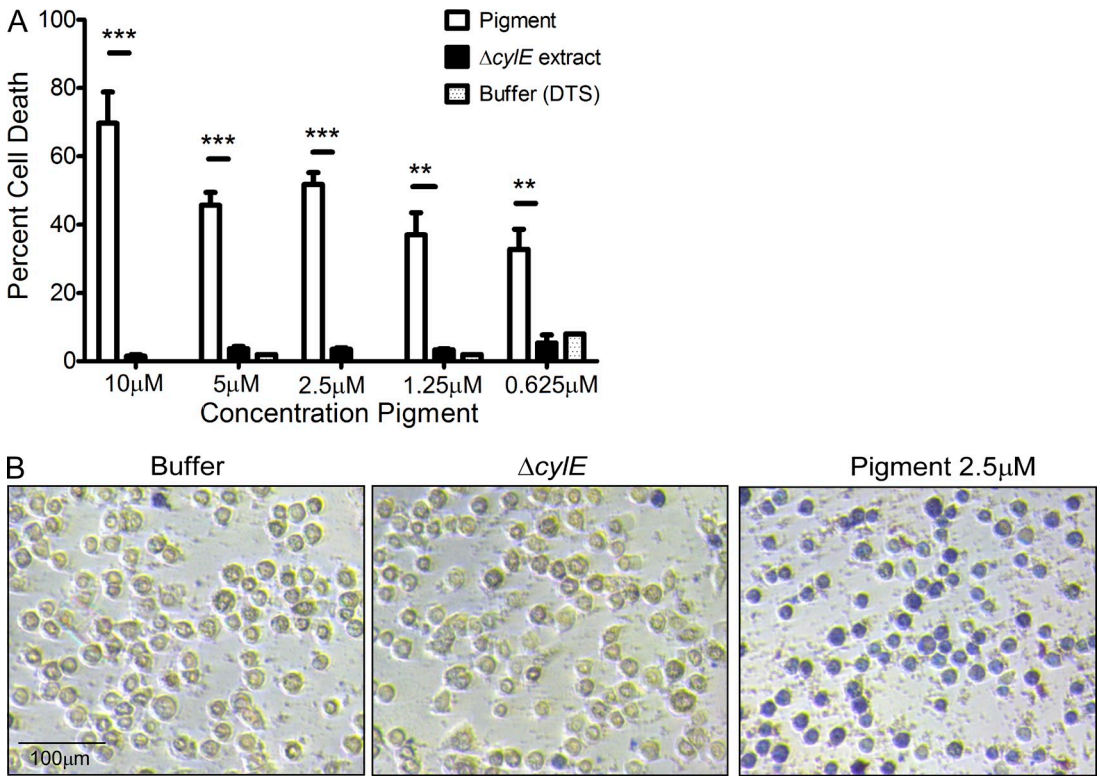

Figure 8. The GBS pigment is cytotoxic to hAECs. Various concentrations of GBS pigment or an equal amount of control (Δ*cylE* or DTS) were added to hAEC for 4 h followed by trypan blue staining. The experiment was performed twice in triplicate using independent pigment samples and hAECs. (A) Percent cell death represented as the mean and SD of five randomly selected fields (n = 500 cells; **, $P < 0.005$; ***, $P < 0.001$, Student's t test, error bars ± SD). (B) Sample field showing GBS pigment cytotoxicity at 2.5 μM compared with an equivalent amount of controls.

hemolytic titer assay described previously (Nizet et al., 1996). The results shown in Fig. 7 A indicate that the purified pigment possessed hemolytic activity and the effective concentration 50 (EC_{50}; concentration at which 50% of erythrocytes are lysed) corresponded to a pigment concentration of 0.11 μM. The control samples that included buffer alone and extracts from the nonhemolytic Δ*cylE* strain were not pigmented and did not possess hemolytic activity (Fig. 7 A). Second, varying concentrations of purified pigment were spotted on sheep blood agar (SBA) plates, and the results shown in Fig. 7 B indicate that lysis of RBCs is observed in the presence of pigment and not in the Δ*cylE* or buffer controls. Scanning electron micrographs of hRBCs revealed that a brief (8 min) exposure to the GBS pigment induced dramatic alterations in membrane morphology from the usual disc shape of erythrocytes (see buffer and Δ*cylE* control) to that of echinocytes and spheroechinocytes (Fig. 7 C).

The hemolytic activity of the ornithine rhamnolipid is not sensitive to proteinase K

To determine if the hemolytic activity observed with purified pigment could be attributed to a protein toxin, we performed proteinase K digestion of the purified pigment before hemolytic assays. For proteinase K digestion, GBS pigment and control Δ*cylE* extract previously dissolved in DTS was lyophilized, resuspended in proteinase K buffer, and digested in the presence and absence of proteinase K (see Materials and methods for details). Subsequently, hemolytic titer assays were performed on all samples including controls. The results shown in Fig. 7 D indicate that pigment treated with proteinase K had similar hemolytic properties compared with pigment not treated with proteinase K ($P \geq 0.9$). We further performed Fourier transform ion cyclotron resonance tandem mass spectrometry and nuclear magnetic resonance (NMR) on the purified pigment and control Δ*cylE* extract (Figs. S2–S4). A comparison of the MS spectra revealed that peaks at 677.38 m/z and a methylated derivative at 691.46 m/z, characteristic of the GBS pigment, are uniquely present in the purified pigment and not in control Δ*cylE* (Fig. S2). ^{1}H NMR and correlation spectroscopy (COSY) confirms the structure of the pigment and its presence in the pigment from WT (Fig. S3, A and B) and not in the Δ*cylE* control (Fig. S4). Also, SDS-PAGE analysis of purified pigment followed by Ruby staining did not reveal the presence of any protein and LC-MS/MS analysis of tryptic digests of purified pigment only identified peptides corresponding to trypsin and common contaminants in these analyses, i.e., keratin (unpublished data). Collectively, these results indicate that the hemolytic molecule purified from GBS is not a protein, but the ornithine rhamnolipid previously described as granadaene (Rosa-Fraile et al., 2006; Vanberg et al., 2007).

The GBS pigment is cytotoxic to hAECs

To determine if the purified pigment has cytotoxic properties attributed to the function of the previously elusive GBS hemolysin, varying concentrations of purified pigment or buffer and Δ*cylE* controls were added to hAEC followed by trypan blue straining. These results indicate that the purified pigment possesses cytolytic properties, as indicated by increased trypan blue staining indicative of dead cells in the presence of pigment in contrast to buffer or Δ*cylE* controls (Fig. 8, A and B, $P < 0.005$). ELISA assays for cytokines indicated that the purified pigment was unable to induce an inflammatory response in hAEC (unpublished data). These results can be expected because GBS hemolysin/pigment is associated with the bacterial cell surface and is not secreted. These observations indicate that although the purified pigment may induce pore formation similar to other rhamnolipids (Kawai et al., 1982; Sánchez et al., 2010) and polyenes (Knopik-Skrocka and Bielawski, 2002), exposure of host cells to bacterial cell surface associated hemolysin is required for induction of the inflammatory response.

DISCUSSION

This work provides novel evidence that elevated expression of a virulence factor promotes GBS penetration of the amniotic cavity, a critical step in the pathway to preterm birth and fetal injury. Currently, there is no effective vaccine to prevent maternal to infant transmission of GBS. Knowledge of virulence factors associated with preterm birth and neonatal infections will allow for a more informed approach toward strategies for prevention of GBS infections. We have demonstrated that hemolysin promotes GBS invasion of placental cells and that hyper-hemolytic strains are more proficient in disruption of the amniotic barrier and penetration of placental membranes. We predict that environmental changes in the lower genital tract (e.g., neutral pH; Santi et al., 2009) may be sensed by sensor kinases, such as CovS, to alleviate CovR repression, thus triggering an increase in hemolysin expression that mediates ascending GBS infection. Alternatively, mutations in hemolysin regulators such as *covR/S* that potentially arise while GBS is in a commensal niche (e.g., during vaginal colonization) may promote penetration of chorioamnion and invasion of the amniotic cavity. Consistent with this hypothesis, hyper-hemolytic GBS with *covR/S* mutations were isolated from the amniotic fluid, chorioamnion, and cord blood of women who delivered preterm. However, GBS strains that had no mutations in the *covR/S* loci were also recovered from women in preterm labor. Although repression of hemolysin by the CovR/S two component system has been demonstrated in several GBS strains (e.g. A909, COH1, NEM316, 515, 2603v/r, and NCTC10/84; Lamy et al., 2004; Jiang et al., 2005, 2008; Rajagopal et al., 2006; Lin et al., 2009; Santi et al., 2009; Firon et al., 2013) and *covR/S* and *cyl* genes are conserved among all sequenced GBS strains (Glaser et al., 2002; Tettelin et al., 2005), it is likely that additional strain-specific regulators also influence the expression of this important virulence factor. Regulators such as the sensor kinase Stk1 (Rajagopal et al., 2006; Lin et al., 2009) and an Abi-domain protein Abx1 (Firon et al., 2013) influence the expression of *cyl* genes through their interaction with CovR and CovS, respectively. As strains lacking Stk1 or Abx1 exhibit decreased hemolytic activity (Rajagopal et al., 2006; Lin et al., 2009; Firon et al., 2013), increased hemolytic activity observed in the clinical isolates cannot be attributed to the loss of Stk1 or Abx1 and DNA sequence analysis also did not indicate the presence of any mutations in these genes (unpublished data). The complexity of hemolysin regulation is emerging and will be beneficial for a greater understanding of GBS infections associated with preterm premature rupture of membranes (PPROM), preterm delivery (PTD), and neonatal sepsis.

For the first time, we describe the biochemical nature of the GBS hemolysin and elucidate the connection between hemolysis and pigmentation. We show that CylE is necessary but not sufficient for GBS hemolysis and that the ornithine rhamnolipid pigment is hemolytic and cytotoxic. Although a previous study suggested that the GBS hemolysin is likely to be a protein as hemolytic activity diminished due to protease treatment (Marchlewicz and Duncan, 1981), three proteins, including a glycoprotein, copurified with the hemolysin in these prior studies. Given the promiscuity of stabilizers used by the GBS hemolysin (starch, tween, and BSA; Marchlewicz and Duncan, 1980; Tapsall, 1987), we predict that protease digestion of the proteins which copurified with the GBS pigment/hemolysin may have destabilized the pigment leading to the erroneous conclusion that the GBS hemolysin is a protein.

Our finding that an ornithine rhamnolipid is the hemolysin has important implications for GBS disease pathogenesis. As the GBS hemolysin/pigment is a surface-associated toxin, we predict that the cytotoxic effects are primarily extracellular but that the toxin also mediates host cell lysis when bacteria are internalized into host cells. These cytotoxic properties contribute to barrier failure, thus promoting bacterial dissemination within the host. Hemolytic GBS also induce a strong immune response (Fig. 2, A and B; Fig. 3 C), which plays an important role in its disease pathogenesis. However, specific host immune pathways that respond to this virulence factor remain undefined (Nizet et al., 1996; Doran et al., 2002; Henneke et al., 2002; Lembo et al., 2010; Bebien et al., 2012). With the identification, purification, and biochemical characterization of the GBS hemolysin as the ornithine rhamnolipid pigment, key mechanisms of host immune activation can now be addressed. Such studies will provide critical insight necessary for preventive strategies against GBS infections. Although vaccines that target surface proteins was shown to provide protection against GBS in mouse models of infection (Maione et al., 2005), protein-based vaccines cannot neutralize the effect of this lipid toxin. A previous attempt to raise anti-sera to crude extracts of the GBS hemolysin was unsuccessful (Dal and Monteil, 1983) and is consistent with the notion that lipids typically do not elicit an antibody response. However, therapeutic measures designed to inhibit biosynthesis of the ornithine rhamnolipid pigment or its function may prove effective.

Although ornithine-containing lipids are widely known in bacteria (Geiger et al., 2010) and a few have hemolytic or hemagglutinating properties (Kawai et al., 1982; Häussler et al.,

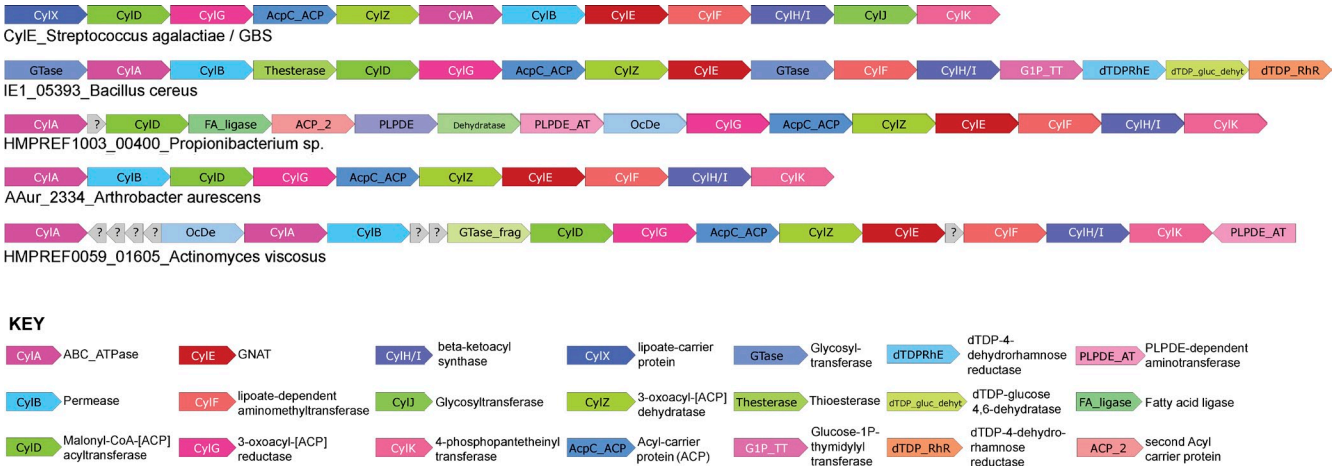

Figure 9. The rhamnolipid biosynthetic Cyl operon is conserved in several bacteria. Genes within operons are shown as box arrows with the arrowhead pointing in the 5′ to the 3′ direction of the coding strand. Bacteria representing a subset of the species containing the Cyl operon are shown (for a detailed list, also see CylE homologues in Fig. S1). Gene and species names are indicated below the operons and gene name abbreviations are expanded in the key provided below.

1998; Sánchez et al., 2010), their role in virulence of bacterial pathogens is not fully appreciated. Orthologs of the *cyl* operon are present in other bacterial species including opportunistic human and insect pathogens such *Bacillus cereus*, *Bacillus thuringiensis*, *Paenibacillus larvae*, and actinobacteria such as *Actinomyces viscosus*, *Kitasatospora setae*, Arthrobacter species, and Propionibacterium species (Fig. 9). In these organisms, the core *cyl* operon containing genes for fatty acid and ornithine biosynthesis and their amidoligation are strongly conserved. Also, *P. jensenii* was described to produce a pigment similar to the GBS granadaene (Vanberg et al., 2007). Given their ubiquitous nature, our findings have significant implication in the classification of bacteria that encode pigments with hemolytic and cytolytic properties. In summary, our work shows that GBS virulence and its transition from commensal to invasive niches hinges on its ability to regulate the expression of a key virulence factor which we describe is a hemolytic ornithine lipid.

MATERIALS AND METHODS

Human subjects. Written informed patient consent for donation of normal, term placentas immediately after cesarean delivery from women without labor was obtained with approval from the University of Washington Institutional Review Board (protocol #34004). GBS clinical isolates from amniotic fluid, chorioamnion, and/or cord blood were obtained from women enrolled with preterm labor and intact membranes at ≤34 wk gestation at the University of Washington Medical Center, Swedish Medical Center, and Virginia Mason Medical Center (Seattle, Washington) between June 25, 1991 and June 30, 1997. This cohort was previously described (Hitti et al., 1997), the University of Washington Institutional Review Board approved the study (protocol #25739), and all participants provided written informed consent. Written informed patient consent for donation of human blood was obtained with approval from the Seattle Children's Research Institute Institutional Review Board (protocol #11117).

Bacterial isolates The WT GBS strains used in this study COH1 and A909 are clinical isolates obtained from infected human newborns. (Lancefield et al., 1975; Martin et al., 1988). COH1 belongs to the hypervirulent MLST-ST17 clone of GBS serotype III associated with severe neonatal infections (Musser et al., 1989). The Δ*cylE*, Δ*covR*, and Δ*covR*Δ*cylE* mutants were derived from COH1 and A909 using methods previously described (Rajagopal et al., 2006; Lembo et al., 2010). The Δ*covS* mutant was derived using methods previously described (Jiang et al., 2005). Routine cultures of GBS were grown in Tryptic Soy Broth (TSB; Difco Laboratories) at 37°C in 5% CO_2, and routine cultures of *E. coli* were performed in Luria-Bertani Broth (LB; Difco Laboratories) at 37°C. Cell growth was monitored at 600 nm. Antibiotics were added at the following concentrations when necessary: for GBS, 1 µg/ml erythromycin, 300 µg/ml spectinomycin, 1,000 µg/ml kanamycin, and 2.5–5 µg/ml chloramphenicol; for *E. coli*, 300 µg/ml erythromycin, 50 µg/ml spectinomycin, 50 µg/ml kanamycin, and 10 µg/ml chloramphenicol. Antibiotics and other chemicals were purchased from Sigma-Aldrich, unless mentioned otherwise. Cell culture media was purchased from Mediatech Inc. All GBS mutants used in this study had similar growth rates compared with isogenic WT in the media used for cell culture and ex vivo experiments (DMEM containing 1% FCS). Restriction enzymes were purchased from Fermentas, and primers were purchased from Sigma-Aldrich. RNA isolation and qRT-PCR for analysis of GBS gene expression was performed as described previously (Lembo et al., 2010). GBS pictures shown on Red Blood Agar and Granada Media were captured using a digital SLR camera (EOS Rebel XSi 12.2MP; Cannon) with an 18–55 mm zoom lens and processed using Photoshop CS2 (version 9; Adobe) and compiled using Canvas 9 (version 9.0.4; Deneba).

Construction of GBS Δ*cylX-K* and complementing plasmids. Approximately 1 kb of DNA located upstream of *cylX* and 1 kb of DNA located downstream of *cylK* were amplified using high fidelity PCR (Invitrogen) and primer pairs dCylopupF and dCylopupR, and dCylop dnF and dCylopdnR, respectively. The gene conferring kanamycin (Ω *km-2*) resistance was also amplified using high-fidelity PCR from pCIV2 (Okada et al., 1993) for allelic replacement of *cylX-K*, using primers dCylkanF and dCylkanR. Subsequently, strand overlap extension PCR (Horton, 1995) was performed to introduce the antibiotic resistance gene (Ω *km-2*) between the flanking regions of *cylX-K* described above. The PCR fragment was then ligated into the temperature-sensitive vector pHY304 (Chaffin et al., 2000) and the resulting plasmid was electroporated into GBS WT as described previously (Rajagopal et al., 2003). Selection and screening for the double crossover mutant was performed as previously described (Rajagopal et al., 2003). PCR was used to verify the presence of Ω *km-2* and the absence of *cylX-K*. The genes encoding *cylE*, *cylABE*, *covR*, and *covS* were amplified using high-fidelity PCR using primer pairs CylEF and CylER, CylABEF and CylABER, CovRF and CovRR, and CovSF and CovSR, respectively. The PCR fragments were digested with restriction enzymes present on the primer sequences and then

cloned into the multiple cloning site of the GBS complementation vector pDC123 downstream to the constitutive promoter as described previously (Chaffin and Rubens, 1998; Rajagopal et al., 2003). The complementing plasmids were then electroporated into GBS Δ*cylE*, Δ*cylX-K*, Δ*covS*, and Δ*covR* using methods previously described (Rajagopal et al., 2003). Site-directed mutants were generated using the QuikChange Site-Directed mutagenesis kit (QIAGEN) with the complementing pCovS plasmid as the template and primers CovS200F & CovS200R for pCovS220Stop and primers CovSV343MF & CovSV343MR for pCovSV343M. GBS with chromosomal mutations in CovR/S loci was obtained using methods described previously (Lin et al., 2009). DNA sequencing was performed to confirm the presence of the desired mutations.

Derivation of human amniotic epithelium. Primary hAECs were isolated and cultured from normal, term placentas obtained immediately after cesarean delivery from women without labor as previously described (Sun et al., 2003). In brief, the amnion was peeled from the chorion, and the amnion tissue was washed with PBS and digested with trypsin (Worthington Biochemical Corp.) and DNase (Sigma-Aldrich) as previously described (Sun et al., 2003). Subsequently, the trypsin digestion media was centrifuged and cell pellets were resuspended in DMEM and loaded onto pre-prepared discontinuous Percoll (GE Healthcare) gradients (5, 20, 40, and 60%, respectively), and the gradients were centrifuged as previously described (Sun et al., 2003). A single band of cells at ∼20% Percoll concentration was collected, diluted in media to a density of 10^6 cells/ml, and cultured as previously described (Sun et al., 2003).

Infection assays. Three to four independent placentas were used and all experiments were performed in triplicate. Adherence and invasion of GBS WT COH1 or A909 and isogenic Δ*cylE*, Δ*covR*, Δ*covS*, and Δ*covR*Δ*cylE* mutants to hAEC were performed as previously described (Nizet et al., 1997; Winram et al., 1998). In brief, GBS strains grown to mid-log phase (∼10^8 CFU/ml; OD_{600} = 0.3) were washed in PBS, resuspended in DMEM with 10% FBS, and used to infect hAEC monolayers at a multiplicity of infection of 1. For adherence assays, the infection was performed for a period of 2 h after which the bacteria were enumerated using methods previously described (Nizet et al., 1997; Winram et al., 1998). For invasion assays, 100 μg/ml gentamicin and 5 μg/ml penicillin was added to each well at 2 h after infection and the plates were incubated for an additional 2 h to kill extracellular and surface-adherent bacteria; subsequently, intracellular bacteria were released using trypsin-EDTA (Gibco) and Triton X-100 and bacteria were serially diluted and enumerated as previously described (Nizet et al., 1997; Winram et al., 1998).

Expression of inflammatory mediators. Three independent placentas were used and all experiments were performed in triplicate. hAECs were cultured, washed, and infected with GBS strains as described above. Subsequently, total RNA was isolated from hAEC monolayers using the RNeasy miniprep kit (QIAGEN) according to the manufacturer's protocol and digested with DNase I to remove contaminating genomic DNA. Expression of inflammatory mediators in human amniotic epithelium was determined using qRT-PCR as described previously (Lembo et al., 2010). Supernatants from GBS-infected hAEC were collected, centrifuged to remove bacteria, and Luminex bead assays (Millipore) were performed using methods described by the manufacturer to evaluate cytokine levels.

Western blots. hAECs were grown to confluence and infected with GBS at a multiplicity of infection of 1 for a period of 4 h. Uninfected cells were included as controls. Subsequently, hAECs were washed, digested with trypsin, and centrifuged. The NE-PER kit (Thermo Fisher Scientific) was used for stepwise separation and preparation of cytoplasmic and nuclear extracts from infected hAEC as per manufacturer's instructions. Equal amounts (10 μg) of cytoplasmic and nuclear extracts were subjected to 7.5% SDS-PAGE followed by Western blotting. The membrane was blocked in 1:1 Odyssey blocking buffer (Li-Cor Biosciences) in PBS and then incubated at 4°C overnight with a 1:200 dilution of primary NF-κB p65 antibody (Santa Cruz Biotechnology). Secondary antibody Alexa Fluor 680 anti–mouse (Life Technologies) was added at a 1:1,000 dilution. After several washes, the membrane was visualized with the Odyssey Li-Cor infrared imager (Li-Cor Biosciences).

Barrier integrity analysis. Changes in transepithelial electrical resistance across hAEC monolayers were measured in real time using ECIS (Giaever and Keese, 1993) with an ECIS ZTheta Instrument and 8W10E+ arrays (Applied BioPhysics). hAEC monolayers were established on gold-plated electrodes in 8-well array slides attached to a computer-operated sensing apparatus to allow measurements in real time. Monolayers were then infected with the GBS strains at 10^5 CFU/well and the system measured the cell membrane capacitance (Cm), the resistance from the cell-electrode interaction (α), and the barrier function properties of the cell monolayer (Rb). Deconvolution of the overall ECIS signal into these parameters is performed by the ECIS software by fitting the mathematical model derived by Giaever and Keese (1991) to the experimental data by least-square optimization procedures. Uninfected wells served as controls for background levels of electrical resistance. Data are represented as a change in resistance as a proportion of the control over time as described previously (Lembo et al., 2010). A representative of three independent experiments is shown.

Ex vivo placental model. Intact chorioamniotic membranes obtained immediately after normal, cesarean delivery were rinsed in sterile saline solution and placed over an inverted, upper chamber of a Transwell System (Corning Inc.) from which the original polycarbonate membrane was previously removed as previously described (Zaga-Clavellina et al., 2007). Sterile silicone rubber rings were used to hold the placental membranes in place. Thus, when the transwell is inserted, the choriodecidua faces the upper chamber and the amniotic epithelium faces the lower chamber as previously described (Zaga-Clavellina et al., 2007). Care was taken to during the entire procedure so that there were no tears or rips on the placental membranes mounted on the transwell. The explants were stabilized in media for a period of 48 h. Six independent placentas/chorioamniotic membranes were used in these assays. Uninfected placenta was also included as a control in each experiment. For infection of chorioamnion, GBS strains were grown to an $O.D_{600}$ of 0.3, washed twice in PBS, and ∼10^7 CFU in a final volume of 1 ml DMEM was added to the upper chamber. At 24 h after infection, media (DMEM) from the lower chamber was removed and processed for bacterial enumeration and expression of cytokines. For bacterial enumeration, aliquots of the media were serially diluted and plated on TSA plates. For analysis of inflammatory mediators, aliquots of media were analyzed using ELISA or the Luminex bead assay as described by the manufacturer (R&D Systems or Millipore). For microscopy, infected chorioamniotic membranes were fixed in 10% phosphate buffered formalin at 4°C overnight and stored in 70% ethanol. The membranes were subsequently embedded in paraffin, sectioned, and stained using the Gram-Twort stain as previously described (Stevens and Bancroft, 1977). Images were captured in bright field using the DM4000B Fluorescent upright microscope (Leica) under 10, 40, and 100× magnifications. The microscope was attached to a DFC310FX camera (Leica) and the acquisition software used was the Leica application suite (version 4.0.0). A representative image from experiments with six independent placentas with similar results is shown. As controls for bacterial migration, transwells were also mounted with either chorion alone or amnion alone. In brief, the amnion was peeled from the chorion and individual membranes were mounted over the transwell such that their orientation was maintained, i.e., the inner chamber represented the choriodecidual side for chorionic transwells or amniotic mesoderm for amniotic transwells. Infection with GBS strains was performed as described above.

Purification and characterization of the ornithine rhamnolipid pigment. GBS pigment was purified as previously described (Rosa-Fraile et al., 2006) with some modifications. In brief, WT GBS were grown at 37°C in New Granada Media (de la Rosa et al., 1992) until the broth turned red (48–72 h). Bacterial cells were pelleted, washed three times with distilled water and twice with DMSO. The cell pellet was then resuspended in DMSO:0.1% TFA overnight to extract the pigment, cell debris was pelleted, and the supernatant containing the pigment was saved. The above

process was repeated until the supernatant obtained from GBS cells was clear. Pigment was then precipitated by addition of 25% NH_4OH to a final concentration of 0.25% as previously described (Vanberg et al., 2007). Precipitated pigment was washed three times with HPLC grade water and twice in DMSO, redissolved in DMSO:0.1%TFA, and purified using a Sephadex LH-20 (GE Healthcare) column as previously described (Rosa-Fraile et al., 2006; Vanberg et al., 2007). Fractions containing purified pigment were pooled and precipitated with NH_4OH (Scientific Products) as described above, washed three times with HPLC grade water, twice with DMSO, and lyophilized. As a control, GBSΔ*cylE* was also grown in New Granada Media and pigment extraction protocol was followed as described above. For NMR analysis, purified pigment or control Δ*cylE* samples were resuspended in DMSO-d_6:0.1% *d*-TFA (Sigma-Aldrich). ^1H,^{13}C, ^1H-COSY NMR experiments were performed at 298K on a Bruker AV-500 NMR Spectrometer. Residual DMSO-d_5 was used to calibrate chemical shifts. For MS experiments, lyophilized pigment or control Δ*cylE* samples were dissolved in DMSO:0.1%TFA and analyzed by Fourier Transform Ion Cyclotron Resonance mass spectrometry on a Bruker AutoFlex APEX Qe 47e instrument. For hemolytic and cytotoxic assays, lyophilized pigment or control Δ*cylE* extract was dissolved in DTS to a final concentration of 1mM. The samples were incubated overnight at room temperature in the dark before use.

Hemolytic titer assays was performed using methods described with some modifications (Nizet et al., 1996). In brief, twofold serial dilutions of purified pigment or control Δ*cylE* extract in DTS was performed in PBS + 0.2% glucose in a final volume of 100 µl. These samples were then incubated with 100 µl of heparin-treated hRBCs (1%) in 96-well plates at 37°C for 1 h, after which the plates were spun for 4 min at 3,000 *g* to pellet unlysed hRBC. The supernatants were transferred to a replica 96-well plate and hemoglobin release was measured by recording the absorbance at 420 nm. Positive and negative controls included wells that contained hRBC with 0.1% SDS or PBS, respectively. Solvent control for each pigment concentration was included in the analysis. The effective concentration 50 is the concentration of pigment that produces 50% hemoglobin release compared with the SDS control and was determined using non linear regression. The experiment was performed in triplicate using three independent preparations of purified pigment.

For proteinase K treatment of the pigment before hemolytic assays, pigment and control Δ*cylE* samples in DTS was lyophilized and dissolved in proteinase K buffer (20 mM Tris, pH 8.0, and 1 mM $CaCl_2$). Each sample was divided into two and proteinase K was added at a final concentration of 0.25 mg/ml, as previously described (Vanberg et al., 2007), to one of the aliquots and all samples were incubated at 37°C for 1 h. Hemolytic titer assays were then performed on pigment and control samples that were treated with and without proteinase K. Buffer controls were also included. The activity of proteinase K used in these experiments was confirmed by digesting 100 µg BSA with 0.25 mg/ml proteinase K at 37°C for 1 h followed by 12% SDS-PAGE and SYPRO Ruby staining.

Scanning electron microscopy. Erythrocytes from 0.5 ml of human blood was centrifuged, washed twice with PBS, and resuspended in 5 ml PBS. Erythrocytes were then treated with 12.5 µM of pigment or an equivalent amount of controls (DTS or Δ*cylE* extract) for 8 min at 37°C. Subsequently, the samples were centrifuged at 4°C and the supernatant was discarded. The pellet was resuspended in 0.5 ml of 1/2 Karnovsky's Fixative and incubated overnight at room temperature. Samples were then prepared for scanning electron microscopy as previously described (Sánchez et al., 2010). Images were captured using a JEOL 5800 Scanning Electron Microscope equipped with a JEOL Orion Digital Acquisition System. The experiment was performed twice using independent pigment preparations.

Cytotoxicity assays. hAECs cultured in 96-well plates (10^5 cells/well) for 24 h were treated with known concentrations of pigment or equivalent amounts of control Δ*cylE* extract or DTS for a period of 4 h. Subsequently, the media was removed and hAECs were treated with 0.2% trypan blue for 2 min. Cells were washed with PBS and were immediately observed and imaged under a DMI6000B inverted microscope (Leica) and images were captured at 10 and 40× magnifications. The microscope was equipped with a DFC310FX (Leica) camera and the acquisition software used was the Leica application suite, version 4.0.0. Data are reported as the mean and SD of five fields per well.

Statistical analysis. The unpaired, two tailed Students *t* test, Mann-Whitney test, Wilcoxon's matched pairs rank test was used to estimate differences as appropriate, and a value of $P < 0.05$ was considered significant. The nonlinear regression analysis was used to estimate EC_{50} concentration. These tests were performed using Prism for Windows (version 5.0; GraphPad Software).

Online supplemental material. Table S1 lists primers used in this study. Fig. S1 shows the alignment of CylE to known N-acyltransferases. Fig. S2 shows the overlay of mass spectra of purified pigment and control Δ*cylE* extracts. Fig. S3 indicates ^1H chemical shifts and ^1H-^1H COSY NMR of the purified GBS pigment. NMR of control Δ*cylE* extract is shown in Fig. S4. Online supplemental material is available at http://www.jem.org/cgi/content/full/jem.20122753/DC1.

We thank Dr. Victor Nizet for the GBSΔ*cylE* strain, Dr. David Eschenbach for his input, Dr. Sophia Lannon and Evangelyn Nwakapora for assistance in placenta collection, Dr. Kang Sun for helping with derivation of hAEC, Kathy Agnew for isolation of GBS clinical isolates, Dr. Liza Cox for help with microscopy, and Nyugen Thao-Binh Tran, Jessica Klein, and Hannah Miller for technical assistance. The authors are grateful to Christian Renken (Applied Biophysics) for assistance with ECIS. We thank Dr. Paul Miller and Dale Whittington for assistance with NMR and MS analyses, respectively. We also thank Dr. Toni Kline for her expertise with interpretation of the NMR. Histology was performed using the Histology and Imaging Core at the University of Washington.

This work was supported by funding from the National Institutes of Health (NIH) grants R01AI100989 to L. Rajagopal and K.M. Adams Waldorf, R01AI070749 to L. Rajagopal, and K08AI067910 to K.M. Adams Waldorf. This work was also supported by funding from the March of Dimes grant 21-FY08-562 and 21-FY06-77 to K.M. Adams Waldorf. Support for K. Burnside was provided by the NIH training grant (5 T32 HD007233-29, PI: Lisa Frenkel). Support for C. Whidbey was provided by the NIH training grant (T32 AI07509, PI: Lee Ann Campbell). L.M. Iyer and L. Aravind are supported by intramural funds from NLM, NIH. The Cuyamaca Foundation also provided support for this work. We are grateful to the human subjects who participated in these studies. The study on women in preterm labor from where GBS clinical isolates were obtained was funded by R01AI31871.

The authors have no conflicting financial interests.

Submitted: 12 December 2012
Accepted: 1 May 2013

REFERENCES

Ala-Kokko, T.I., P. Myllynen, and K. Vahakangas. 2000. Ex vivo perfusion of the human placental cotyledon: implications for anesthetic pharmacology. *Int. J. Obstet. Anesth.* 9:26–38. http://dx.doi.org/10.1054/ijoa.1999.0312

Bebien, M., M.E. Hensler, S. Davanture, L.C. Hsu, M. Karin, J.M. Park, L. Alexopoulou, G.Y. Liu, V. Nizet, and T. Lawrence. 2012. The pore-forming toxin β hemolysin/cytolysin triggers p38 MAPK-dependent IL-10 production in macrophages and inhibits innate immunity. *PLoS Pathog.* 8:e1002812. http://dx.doi.org/10.1371/journal.ppat.1002812

Behrman, R.E., and A.S. Butler, editors. 2007. Preterm Birth: Causes, Consequences and Prevention. The National Academies Press, Washington, D.C. 792 pp.

Bobitt, J.R., and W.J. Ledger. 1977. Unrecognized amnionitis and prematurity: a preliminary report. *J. Reprod. Med.* 19:8–12.

Bourne, G.L. 1960. The microscopic anatomy of the human amnion and chorion. *Am. J. Obstet. Gynecol.* 79:1070–1073.

Chaffin, D.O., and C.E. Rubens. 1998. Blue/white screening of recombinant plasmids in Gram-positive bacteria by interruption of alkaline phosphatase gene (phoZ) expression. *Gene.* 219:91–99. http://dx.doi.org/10.1016/S0378-1119(98)00396-5

Chaffin, D.O., S.B. Beres, H.H. Yim, and C.E. Rubens. 2000. The serotype of type Ia and III group B streptococci is determined by the polymerase gene within the polycistronic capsule operon. *J. Bacteriol.* 182:4466–4477. http://dx.doi.org/10.1128/JB.182.16.4466-4477.2000

Dal, M.-C., and H. Monteil. 1983. Hemolysin produced by group B *Streptococcus agalactiae*. *FEMS Microbiol. Lett.* 16:89–94. http://dx.doi.org/10.1111/j.1574-6968.1983.tb00265.x

de la Rosa, M., M. Perez, C. Carazo, L. Pareja, J.I. Peis, and F. Hernandez. 1992. New Granada Medium for detection and identification of group B streptococci. *J. Clin. Microbiol.* 30:1019–1021.

Doran, K.S., J.C. Chang, V.M. Benoit, L. Eckmann, and V. Nizet. 2002. Group B streptococcal beta-hemolysin/cytolysin promotes invasion of human lung epithelial cells and the release of interleukin-8. *J. Infect. Dis.* 185:196–203. http://dx.doi.org/10.1086/338475

Doran, K.S., E.J. Engelson, A. Khosravi, H.C. Maisey, I. Fedtke, O. Equils, K.S. Michelsen, M. Arditi, A. Peschel, and V. Nizet. 2005. Blood-brain barrier invasion by group B Streptococcus . proper cell-surface anchoring of lipoteichoic acid. *J. Clin. Invest.* 115:2499–2507. http://dx.doi.org/10.1172/JCI23829

Firon, A., A. Tazi, V. Da Cunha, S. Brinster, E. Sauvage, S. Dramsi, D.T. Golenbock, P. Glaser, C. Poyart, and P. Trieu-Cuot. 2013. The Abi-domain protein Abx1 interacts with the CovS histidine kinase to control virulence gene expression in group B Streptococcus. *PLoS Pathog.* 9:e1003179. http://dx.doi.org/10.1371/journal.ppat.1003179

Forquin, M.P., A. Tazi, M. Rosa-Fraile, C. Poyart, P. Trieu-Cuot, and S. Dramsi. 2007. The putative glycosyltransferase-encoding gene *cylJ* and the group B Streptococcus (GBS)-specific gene *cylK* modulate hemolysin production and virulence of GBS. *Infect. Immun.* 75:2063–2066. http://dx.doi.org/10.1128/IAI.01565-06

Geiger, O., N. González-Silva, I.M. López-Lara, and C. Sohlenkamp. 2010. Amino acid-containing membrane lipids in bacteria. *Prog. Lipid Res.* 49:46–60. http://dx.doi.org/10.1016/j.plipres.2009.08.002

Giaever, I., and C.R. Keese. 1991. Micromotion of mammalian cells measured electrically. *Proc. Natl. Acad. Sci. USA.* 88:7896–7900. http://dx.doi.org/10.1073/pnas.88.17.7896

Giaever, I., and C.R. Keese. 1993. A morphological biosensor for mammalian cells. *Nature.* 366:591–592. http://dx.doi.org/10.1038/366591a0

Glaser, P., C. Rusniok, C. Buchrieser, F. Chevalier, L. Frangeul, T. Msadek, M. Zouine, E. Couvé, L. Lalioui, C. Poyart, et al. 2002. Genome sequence of *Streptococcus agalactiae*, a pathogen causing invasive neonatal disease. *Mol. Microbiol.* 45:1499–1513. http://dx.doi.org/10.1046/j.1365-2958.2002.03126.x

Goldenberg, R.L., J.C. Hauth, and W.W. Andrews. 2000. Intrauterine infection and preterm delivery. *N. Engl. J. Med.* 342:1500–1507. http://dx.doi.org/10.1056/NEJM200005183422007

Gonzalez, M.R., M. Bischofberger, L. Pernot, F.G. van der Goot, and B. Frêche. 2008. Bacterial pore-forming toxins: the (w)hole story? *Cell. Mol. Life Sci.* 65:493–507. http://dx.doi.org/10.1007/s00018-007-7434-y

Gotsch, F., R. Romero, J.P. Kusanovic, S. Mazaki-Tovi, B.L. Pineles, O. Erez, J. Espinoza, and S.S. Hassan. 2007. The fetal inflammatory response syndrome. *Clin. Obstet. Gynecol.* 50:652–683. http://dx.doi.org/10.1097/GRF.0b013e31811ebef6

Gottschalk, B., G. Bröker, M. Kuhn, S. Aymanns, U. Gleich-Theurer, and B. Spellerberg. 2006. Transport of multidrug resistance substrates by the *Streptococcus agalactiae* hemolysin transporter. *J. Bacteriol.* 188:5984–5992. http://dx.doi.org/10.1128/JB.00768-05

Gravett, M.G., C.E. Rubens, and T.M. Nunes; GAPPS Review Group. 2010. Global report on preterm birth and stillbirth (2 of 7): discovery science. *BMC Pregnancy Childbirth.* 10:S2. http://dx.doi.org/10.1186/1471-2393-10-S1-S2

Häussler, S., M. Nimtz, T. Domke, V. Wray, and I. Steinmetz. 1998. Purification and characterization of a cytotoxic exolipid of *Burkholderia pseudomallei*. *Infect. Immun.* 66:1588–1593.

Henneke, P., O. Takeuchi, R. Malley, E. Lien, R.R. Ingalls, M.W. Freeman, T. Mayadas, V. Nizet, S. Akira, D.L. Kasper, and D.T. Golenbock. 2002. Cellular activation, phagocytosis, and bactericidal activity against group B streptococcus involve parallel myeloid differentiation factor 88-dependent and independent signaling pathways. *J. Immunol.* 169:3970–3977.

Hensler, M.E., G.Y. Liu, S. Sobczak, K. Benirschke, V. Nizet, and G.P. Heldt. 2005. Virulence role of group B Streptococcus beta-hemolysin/cytolysin in a neonatal rabbit model of early-onset pulmonary infection. *J. Infect. Dis.* 191:1287–1291. http://dx.doi.org/10.1086/428946

Hillier, S.L., J. Martius, M. Krohn, N. Kiviat, K.K. Holmes, and D.A. Eschenbach. 1988. A case-control study of chorioamnionic infection and histologic chorioamnionitis in prematurity. *N. Engl. J. Med.* 319:972–978. http://dx.doi.org/10.1056/NEJM198810133191503

Hillier, S.L., M.A. Krohn, N.B. Kiviat, D.H. Watts, and D.A. Eschenbach. 1991. Microbiologic causes and neonatal outcomes associated with chorioamnion infection. *Am. J. Obstet. Gynecol.* 165:955–961. http://dx.doi.org/10.1016/0002-9378(91)90447-Y

Hitti, J., M.A. Krohn, D.L. Patton, P. Tarczy-Hornoch, S.L. Hillier, E.M. Cassen, and D.A. Eschenbach. 1997. Amniotic fluid tumor necrosis factor-alpha and the risk of respiratory distress syndrome among preterm infants. *Am. J. Obstet. Gynecol.* 177:50–56. http://dx.doi.org/10.1016/S0002-9378(97)70437-X

Horton, R.M. 1995. PCR-mediated recombination and mutagenesis. SOEing together tailor-made genes. *Mol. Biotechnol.* 3:93–99. http://dx.doi.org/10.1007/BF02789105

Hutson, J.R., F. Garcia-Bournissen, A. Davis, and G. Koren. 2011. The human placental perfusion model: a systematic review and development of a model to predict in vivo transfer of therapeutic drugs. *Clin. Pharmacol. Ther.* 90:67–76. http://dx.doi.org/10.1038/clpt.2011.66

Jiang, S.M., M.J. Cieslewicz, D.L. Kasper, and M.R. Wessels. 2005. Regulation of virulence by a two-component system in group B streptococcus. *J. Bacteriol.* 187:1105–1113. http://dx.doi.org/10.1128/JB.187.3.1105-1113.2005

Jiang, S.M., N. Ishmael, J. Dunning Hotopp, M. Puliti, L. Tissi, N. Kumar, M.J. Cieslewicz, H. Tettelin, and M.R. Wessels. 2008. Variation in the group B Streptococcus CsrRS regulon and effects on pathogenicity. *J. Bacteriol.* 190:1956–1965. http://dx.doi.org/10.1128/JB.01677-07

Kawai, Y., A. Moribayashi, and I. Yano. 1982. Ornithine-containing lipid of *Bordetella pertussis* that carries hemagglutinating activity. *J. Bacteriol.* 152:907–910.

Knopik-Skrocka, A., and J. Bielawski. 2002. The mechanism of the hemolytic activity of polyene antibiotics. *Cell. Mol. Biol. Lett.* 7:31–48.

Lamy, M.C., M. Zouine, J. Fert, M. Vergassola, E. Couve, E. Pellegrini, P. Glaser, F. Kunst, T. Msadek, P. Trieu-Cuot, and C. Poyart. 2004. CovS/CovR of group B streptococcus: a two-component global regulatory system involved in virulence. *Mol. Microbiol.* 54:1250–1268. http://dx.doi.org/10.1111/j.1365-2958.2004.04365.x

Lancefield, R.C., M. McCarty, and W.N. Everly. 1975. Multiple mouse-protective antibodies directed against group B streptococci. Special reference to antibodies effective against protein antigens. *J. Exp. Med.* 142:165–179. http://dx.doi.org/10.1084/jem.142.1.165

Ledger, W.J. 2008. Perinatal infections and fetal/neonatal brain injury. *Curr. Opin. Obstet. Gynecol.* 20:120–124. http://dx.doi.org/10.1097/GCO.0b013e3282f734db

Lembo, A., M.A. Gurney, K. Burnside, A. Banerjee, M. de los Reyes, J.E. Connelly, W.J. Lin, K.A. Jewell, A. Vo, C.W. Renken, et al. 2010. Regulation of CovR expression in Group B Streptococcus impacts blood-brain barrier penetration. *Mol. Microbiol.* 77:431–443. http://dx.doi.org/10.1111/j.1365-2958.2010.07215.x

Lin, W.J., D. Walthers, J.E. Connelly, K. Burnside, K.A. Jewell, L.J. Kenney, and L. Rajagopal. 2009. Threonine phosphorylation prevents promoter DNA binding of the Group B Streptococcus response regulator CovR. *Mol. Microbiol.* 71:1477–1495. http://dx.doi.org/10.1111/j.1365-2958.2009.06616.x

Liu, G.Y., K.S. Doran, T. Lawrence, N. Turkson, M. Puliti, L. Tissi, and V. Nizet. 2004. Sword and shield: linked group B streptococcal beta-hemolysin/cytolysin and carotenoid pigment function to subvert host phagocyte defense. *Proc. Natl. Acad. Sci. USA.* 101:14491–14496. http://dx.doi.org/10.1073/pnas.0406143101

Lukacs, S.L., K.C. Schoendorf, and A. Schuchat. 2004. Trends in sepsis-related neonatal mortality in the United States, 1985-1998. *Pediatr. Infect. Dis. J.* 23:599–603. http://dx.doi.org/10.1097/01.inf.0000131633.74921.90

Maione, D., I. Margarit, C.D. Rinaudo, V. Masignani, M. Mora, M. Scarselli, H. Tettelin, C. Brettoni, E.T. Iacobini, R. Rosini, et al. 2005. Identification of a universal Group B streptococcus vaccine by multiple genome screen. *Science.* 309:148–150. http://dx.doi.org/10.1126/science.1109869

Marchlewicz, B.A., and J.L. Duncan. 1980. Properties of a hemolysin produced by group B streptococci. *Infect. Immun.* 30:805–813.

Marchlewicz, B.A., and J.L. Duncan. 1981. Lysis of erythrocytes by a hemolysin produced by a group B Streptococcus sp. *Infect. Immun.* 34:787–794.

Martin, T.R., C.E. Rubens, and C.B. Wilson. 1988. Lung antibacterial defense mechanisms in infant and adult rats: implications for the pathogenesis of group B streptococcal infections in the neonatal lung. *J. Infect. Dis.* 157:91–100. http://dx.doi.org/10.1093/infdis/157.1.91

Musser, J.M., S.J. Mattingly, R. Quentin, A. Goudeau, and R.K. Selander. 1989. Identification of a high-virulence clone of type III *Streptococcus agalactiae* (group B Streptococcus) causing invasive neonatal disease. *Proc. Natl. Acad. Sci. USA.* 86:4731–4735. http://dx.doi.org/10.1073/pnas.86.12.4731

Naeye, R.L., and E.C. Peters. 1978. Amniotic fluid infections with intact membranes leading to perinatal death: a prospective study. *Pediatrics.* 61:171–177.

Nizet, V. 2002. Streptococcal beta-hemolysins: genetics and role in disease pathogenesis. *Trends Microbiol.* 10:575–580. http://dx.doi.org/10.1016/S0966-842X(02)02473-3

Nizet, V., R.L. Gibson, E.Y. Chi, P.E. Framson, M. Hulse, and C.E. Rubens. 1996. Group B streptococcal beta-hemolysin expression is associated with injury of lung epithelial cells. *Infect. Immun.* 64:3818–3826.

Nizet, V., K.S. Kim, M. Stins, M. Jonas, E.Y. Chi, D. Nguyen, and C.E. Rubens. 1997. Invasion of brain microvascular endothelial cells by group B streptococci. *Infect. Immun.* 65:5074–5081.

Okada, N., R.T. Geist, and M.G. Caparon. 1993. Positive transcriptional control of mry regulates virulence in the group A streptococcus. *Mol. Microbiol.* 7:893–903. http://dx.doi.org/10.1111/j.1365-2958.1993.tb01180.x

Pritzlaff, C.A., J.C. Chang, S.P. Kuo, G.S. Tamura, C.E. Rubens, and V. Nizet. 2001. Genetic basis for the beta-haemolytic/cytolytic activity of group B Streptococcus. *Mol. Microbiol.* 39:236–247. http://dx.doi.org/10.1046/j.1365-2958.2001.02211.x

Puopolo, K.M. 2008. Epidemiology of Neonatal Early-onset Sepsis. *NeoReviews.* 9:e571–e579. http://dx.doi.org/10.1542/neo.9-12-e571

Rajagopal, L., A. Clancy, and C.E. Rubens. 2003. A eukaryotic type serine/threonine kinase and phosphatase in *Streptococcus agalactiae* reversibly phosphorylate an inorganic pyrophosphatase and affect growth, cell segregation, and virulence. *J. Biol. Chem.* 278:14429–14441. http://dx.doi.org/10.1074/jbc.M212747200

Rajagopal, L., A. Vo, A. Silvestroni, and C.E. Rubens. 2006. Regulation of cytotoxin expression by converging eukaryotic-type and two-component signalling mechanisms in *Streptococcus agalactiae*. *Mol. Microbiol.* 62:941–957. http://dx.doi.org/10.1111/j.1365-2958.2006.05431.x

Romero, R., D.T. Brody, E. Oyarzun, M. Mazor, Y.K. Wu, J.C. Hobbins, and S.K. Durum. 1989a. Infection and labor. III. Interleukin-1: a signal for the onset of parturition. *Am. J. Obstet. Gynecol.* 160:1117–1123. http://dx.doi.org/10.1016/0002-9378(89)90172-5

Romero, R., K.R. Manogue, M.D. Mitchell, Y.K. Wu, E. Oyarzun, J.C. Hobbins, and A. Cerami. 1989b. Infection and labor. IV. Cachectin-tumor necrosis factor in the amniotic fluid of women with intraamniotic infection and preterm labor. *Am. J. Obstet. Gynecol.* 161:336–341. http://dx.doi.org/10.1016/0002-9378(89)90515-2

Romero, R., M. Sirtori, E. Oyarzun, C. Avila, M. Mazor, R. Callahan, V. Sabo, A.P. Athanassiadis, and J.C. Hobbins. 1989c. Infection and labor. V. Prevalence, microbiology, and clinical significance of intraamniotic infection in women with preterm labor and intact membranes. *Am. J. Obstet. Gynecol.* 161:817–824. http://dx.doi.org/10.1016/0002-9378(89)90409-2

Romero, R., C. Avila, U. Santhanam, and P.B. Sehgal. 1990. Amniotic fluid interleukin 6 in preterm labor. Association with infection. *J. Clin. Invest.* 85:1392–1400. http://dx.doi.org/10.1172/JCI114583

Romero, R., M. Ceska, C. Avila, M. Mazor, E. Behnke, and I. Lindley. 1991. Neutrophil attractant/activating peptide-1/interleukin-8 in term and preterm parturition. *Am. J. Obstet. Gynecol.* 165:813–820. http://dx.doi.org/10.1016/0002-9378(91)90422-N

Rosa-Fraile, M., J. Rodríguez-Granger, A. Haidour-Benamin, J.M. Cuerva, and A. Sampedro. 2006. Granadaene: proposed structure of the group B Streptococcus polyenic pigment. *Appl. Environ. Microbiol.* 72:6367–6370. http://dx.doi.org/10.1128/AEM.00756-06

Sánchez, M., F.J. Aranda, J.A. Teruel, M.J. Espuny, A. Marqués, A. Manresa, and A. Ortiz. 2010. Permeabilization of biological and artificial membranes by a bacterial dirhamnolipid produced by Pseudomonas aeruginosa. *J. Colloid Interface Sci.* 341:240–247. http://dx.doi.org/10.1016/j.jcis.2009.09.042

Santi, I., R. Grifantini, S.M. Jiang, C. Brettoni, G. Grandi, M.R. Wessels, and M. Soriani. 2009. CsrRS regulates group B Streptococcus virulence gene expression in response to environmental pH: a new perspective on vaccine development. *J. Bacteriol.* 191:5387–5397. http://dx.doi.org/10.1128/JB.00370-09

Spellerberg, B., B. Pohl, G. Haase, S. Martin, J. Weber-Heynemann, and R. Lütticken. 1999. Identification of genetic determinants for the hemolytic activity of *Streptococcus agalactiae* by ISS1 transposition. *J. Bacteriol.* 181:3212–3219.

Spellerberg, B., S. Martin, C. Brandt, and R. Lütticken. 2000. The cyl genes of *Streptococcus agalactiae* are involved in the production of pigment. *FEMS Microbiol. Lett.* 188:125–128. http://dx.doi.org/10.1111/j.1574-6968.2000.tb09182.x

Stevens, A.M., and J.D. Bancroft. 1977. Theory and Practice of Histological Techniques. Churchill Livingstone, Edinburgh. 436 pp.

Sun, K., R. Ma, X. Cui, B. Campos, R. Webster, D. Brockman, and L. Myatt. 2003. Glucocorticoids induce cytosolic phospholipase A2 and prostaglandin H synthase type 2 but not microsomal prostaglandin E synthase (PGES) and cytosolic PGES expression in cultured primary human amnion cells. *J. Clin. Endocrinol. Metab.* 88:5564–5571. http://dx.doi.org/10.1210/jc.2003-030875

Tapsall, J.W. 1987. Relationship between pigment production and haemolysin formation by Lancefield group B streptococci. *J. Med. Microbiol.* 24:83–87. http://dx.doi.org/10.1099/00222615-24-1-83

Tapsall, J.W., and E.A. Phillips. 1991. The hemolytic and cytolytic activity of group B streptococcal hemolysin and its possible role in early onset group B streptococcal disease. *Pathology.* 23:139–144. http://dx.doi.org/10.3109/00313029109060813

Tettelin, H., V. Masignani, M.J. Cieslewicz, C. Donati, D. Medini, N.L. Ward, S.V. Angiuoli, J. Crabtree, A.L. Jones, A.S. Durkin, et al. 2005. Genome analysis of multiple pathogenic isolates of *Streptococcus agalactiae*: implications for the microbial "pan-genome". *Proc. Natl. Acad. Sci. USA.* 102:13950–13955. http://dx.doi.org/10.1073/pnas.0506758102

van Sorge, N.M., D. Quach, M.A. Gurney, P.M. Sullam, V. Nizet, and K.S. Doran. 2009. The group B streptococcal serine-rich repeat 1 glycoprotein mediates penetration of the blood-brain barrier. *J. Infect. Dis.* 199:1479–1487. http://dx.doi.org/10.1086/598217

Vanberg, C., B.F. Lutnaes, T. Langsrud, I.F. Nes, and H. Holo. 2007. *Propionibacterium jensenii* produces the polyene pigment granadaene and has hemolytic properties similar to those of *Streptococcus agalactiae*. *Appl. Environ. Microbiol.* 73:5501–5506. http://dx.doi.org/10.1128/AEM.00545-07

Verani, J.R., L. McGee, and S.J. Schrag; Division of Bacterial Diseases, National Center for Immunization and Respiratory Diseases, Centers for Disease Control and Prevention (CDC). 2010. Prevention of perinatal group B streptococcal disease—revised guidelines from CDC, 2010. *MMWR Recomm. Rep.* 59(RR-10):1–36.

Watts, D.H., M.A. Krohn, S.L. Hillier, and D.A. Eschenbach. 1992. The association of occult amniotic fluid infection with gestational age and neonatal outcome among women in preterm labor. *Obstet. Gynecol.* 79:351–357. http://dx.doi.org/10.1097/00006250-199203000-00005

Weston, E.J., T. Pondo, M.M. Lewis, P. Martell-Cleary, C. Morin, B. Jewell, P. Daily, M. Apostol, S. Petit, M. Farley, et al. 2011. The burden of invasive early-onset neonatal sepsis in the United States, 2005-2008. *Pediatr. Infect. Dis. J.* 30:937–941. http://dx.doi.org/10.1097/INF.0b013e318223bad2

Winram, S.B., M. Jonas, E. Chi, and C.E. Rubens. 1998. Characterization of group B streptococcal invasion of human chorion and amnion epithelial cells In vitro. *Infect. Immun.* 66:4932–4941.

Yoon, B.H., R. Romero, J.S. Park, C.J. Kim, S.H. Kim, J.H. Choi, and T.R. Han. 2000. Fetal exposure to an intra-amniotic inflammation and the development of cerebral palsy at the age of three years. *Am. J. Obstet. Gynecol.* 182:675–681. http://dx.doi.org/10.1067/mob.2000.104207

Zaga-Clavellina, V., G. Garcia-Lopez, H. Flores-Herrera, A. Espejel-Nuñez, A. Flores-Pliego, D. Soriano-Becerril, R. Maida-Claros, H. Merchant-Larios, and F. Vadillo-Ortega. 2007. In vitro secretion profiles of interleukin (IL)-1beta, IL-6, IL-8, IL-10, and TNF alpha after selective infection with *Escherichia coli* in human fetal membranes. *Reprod. Biol. Endocrinol.* 5:46. http://dx.doi.org/10.1186/1477-7827-5-46